Ocean Engineering 117 (2016) 272–291

Contents lists available at ScienceDirect

Ocean Engineering

journal homepage: www.elsevier.com/locate/oceaneng

Assessment of wave characteristics and resource variability at a 1/4-scale wave energy test site in Galway Bay using waverider and high frequency radar (CODAR) data

Reduan Atan [a,b,c], Jamie Goggins [a,b,c,*], Michael Harnett [a,b,c], Pedro Agostinho [d], Stephen Nash [a,b,c]

[a] College of Engineering and Informatics, National University of Ireland, Galway, Ireland
[b] Marine Renewable Energy Ireland (MaREI) Research Centre, Galway, Ireland
[c] Ryan Institute for Environmental, Marine and Energy Research, Galway, Ireland
[d] Qualitas Remos, Lisbon, Portugal

ARTICLE INFO

Article history:
Received 27 October 2015
Received in revised form
25 January 2016
Accepted 13 March 2016

Keywords:
Wave characterisation
Extreme waves
Radar
Galway Bay test site
Wave resource
Wave power

ABSTRACT

This research presents an assessment of wave characteristics at the 1/4 scale wave energy test site in Galway Bay based on (1) data from a waverider buoy from 2009 to 2013 and (2) data from a high frequency radar system (CODAR) from 2011 to 2013. The main objective of this research is to provide an assessment of annual and seasonal wave characteristics and resource variability at a wave energy site. Such assessments are extremely important for wave energy test sites so as to inform the design, optimisation and maintenance of wave energy converters. An approach for classifying operational, high and extreme wave events is presented. The approach is based on percentage of occurrences of particular wave events and can be applied to any site and any wave parameter. In the present research it is separately applied to wave height and wave power. An additional objective is the validation of CODAR wave data for use in assessment of wave height characteristics; this was achieved by comparing CODAR data with waverider data. The research shows that the authors characterisation methodology is easy to apply and unambiguous to interpret. Due to the significant variation in wave parameters at the site from season to season and year to year, operational, high and extreme conditions are presented for the 5-year measurement period, individual years and individual seasons. The research also shows that wave heights determined from CODAR show good agreement with those from a waverider buoy and may be relied upon for accurate site characterisation.

1. Introduction

Waves are generated by the wind blowing over a large stretch of water surface, while extreme waves can be defined as large wave events driven by strong winds (Holthuijsen, 2009). An assessment of wave characteristics at a specific location or area is essential to determine a reliable figure for available resource with regard to wave energy harvesting. In addition, an understanding of wave characteristics and extreme wave events is critical for the engineering design of wave energy convertors (WECs), especially for survivability as severe loadings on WECs can result from extreme wave events (Coe & Neary, 2014). The annual average power resources of deep water waves around the globe is shown in Fig. 1, which is based on hindcast modelled data generated by the National Oceanic and Atmospheric Administration (NOAA) Wave Watch III (NWW3) wind wave model for the 10 year period from 1997 to 2006. It can be seen that the values vary between 30 kW/m and 70 kW/m wave crest with a peak of 100 kW/m in the North-eastern Atlantic Ocean. This practical global wave resource map is in a GIS database that is provided online by Ocean Energy Systems (OES) and can be accessed to identify potential areas of wave power generation (OES, 2015).

Based on Fig. 1, it is clear that Ireland is an area with high wave resources with the annual average wave resource in the range of 60–70 kW/m (Cornett, 2008). The geographical location of Ireland plays a major role in the availability of large wave propagations. Moreover the area is influenced by variable weather conditions (Éireann, 2015). The West coast of Ireland is exposed to the north-eastern Atlantic Ocean (AO), where swell waves can travel more than three thousand miles across the AO before they reach the shores. Based on statistical analysis of the 10-year WorldWaves

* Corresponding author at: College of Engineering and Informatics, National University of Ireland, Galway, Ireland.
E-mail address: Jamie.Goggins@nuigalway.ie (J. Goggins).

http://dx.doi.org/10.1016/j.oceaneng.2016.03.051
0029-8018/

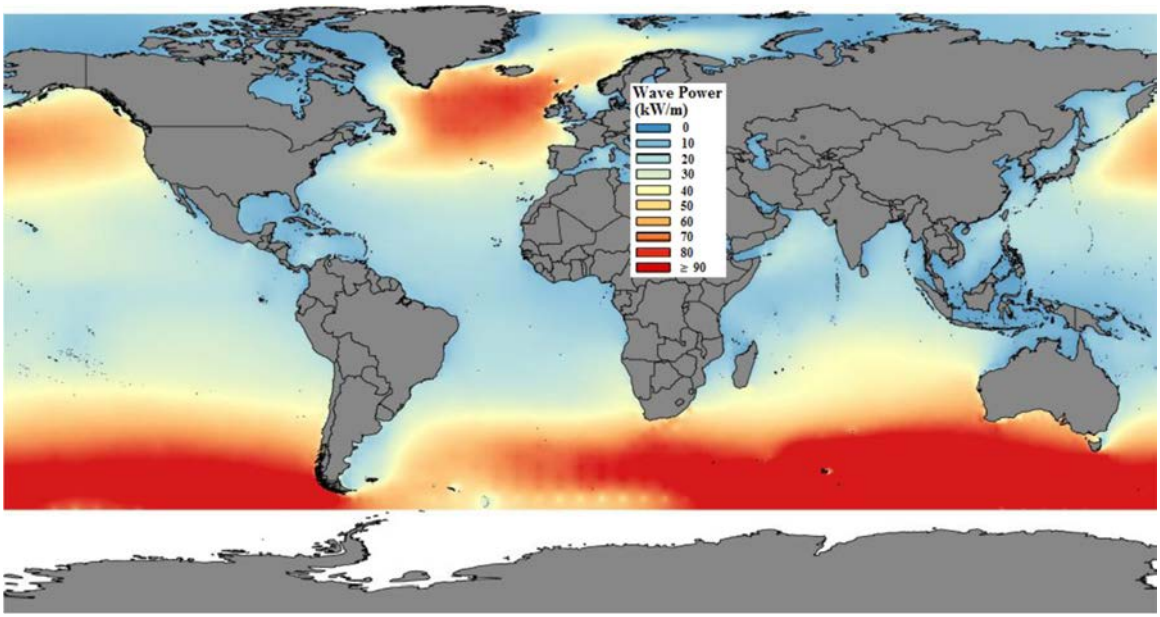

Fig. 1. Global distribution of annual average deep water wave power resources in kilowatts per unit metre (kW/m) (Cornett, 2008).

time series for the period 1997–2006 (Fugro, 2014), annual mean *Hs* values in the Atlantic Ocean are up to 4 m, while off the West coast of Ireland they vary from 2.5 m up to 3.5 m. Thus, it is evident that Ireland, and particularly the West coast of Ireland, is situated in a highly active wave zone. The most recent highest wave recorded in Ireland was 25 m on 12 February 2014, which was measured at Kinsale Energy Gas Platform (−8E, 51.367N), approximately 50 km off the south coast of Cork. The previous record wave height of 23.4 m was measured at Donegal M4 wave buoy off the Northwest coast (−9.992 E, 54.998 N) on 26 January 2014 (Éireann, 2014). A detailed assessment of historical extreme wave events in Ireland is presented in O'Brien et al. (2013), who divide these events into three categories – storm waves, tsunamis waves and rogue waves. The focus of the present research is to investigate the characteristics of wind-generated wave-events, thus only storm waves are examined; tsunamis and rogue waves are not considered.

Given the significant interest in the Irish wave energy resource, there are two existing test sites for wave energy convertors on Ireland's west coast - the Galway Bay test site and the Atlantic Marine Energy Test Site (AMETS) at Belmullet (54.225N, −9.991 W). A third site off the West Coast of Ireland (off Killard in County Clare, near Doonbeg, −9.52E, 52.775N) is the focus of the Westwave demonstration project which aims to deploy five wave energy devices by 2018, moving towards commercialisation of wave power generation. The focus of the assessment in this paper is the Galway Bay 1/4-scale wave energy test site. Galway Bay (in the vicinity area of 53.249N, −9.067 W) is located on the West coast of Ireland and covers approximately 40 km stretch of waters from the inner bay to Aran Islands (see Fig. 3). The area generally experiences a localised wave climate due to the sheltering influences of the surrounding coastlines. The typical conditions of the wave climate result from winds in fetch-limited waters, local geography, bathymetry and some swell waves components coming from the west and southwest sectors (Gulev & Gregorieva, 2006).

Wave resource assessments and wave characteristics analyses can use either measured or modelled wave data. Many different instruments and techniques have been used widely to measure wave data, such as waverider buoys, high frequency radars (HF radar), acoustic Doppler current profilers (ADCP) and traditional wave radars (Pandian et al., 2010). Modelled data may be obtained from different types of wave models, such as NWW3 (Tolman, 1991), SWAN (TUDelft, 2014) and MIKE21 (DHI, 2012), which are all widely used. The main objective of this paper is to provide assessment of wave characteristics and resource variability at the 1/4 scale test site in Galway Bay, Ireland. A set of criteria are presented for identifying operational, high and extreme wave conditions at a site. These criteria are used to classify the site firstly on the basis of wave height and secondly on the basis of available wave power. Understanding operational, high and extreme wave events are conditions at a wave energy test site is vital for the safe and effective design, operation and maintenance of wave energy harvesting devices. The primary dataset used in the assessment is from a waverider buoy situated at the test site. The secondary dataset used is from the Galway Bay HF radar. An additional objective of the research is the validation of HF radar wave data for use in assessment of wave height characteristics by comparison of HF radar data with waverider data.

2. Material and methods

Measured wave data at the 1/4 scale test site were available from (1) the Galway Bay waverider buoy owned and operated by Smartbay Ireland and the Irish Marine Institute and (2) the Galway Bay radar system, a Coastal Ocean Dynamics Applications Radar (CODAR) 25 MHz SeaSonde system owned and operated by National University of Ireland, Galway (NUIG). A preliminary assessment of these data for the period of October to December 2013 was presented in Atan et al. (2014). The present research considers a much longer period of CODAR data from October 2011 to December 2013, while waverider data covers January 2009 to December 2013.

The CODAR mast is located on Spiddal pier as shown in Fig. 2. Radar data is collected for 30 individual bins or range cells (RCs), 0.3 km wide, which extend radially from an origin at Spiddal pier (−9.309E, 53.240N) to a distance of 9 km offshore. Wave parameters measured by CODAR include significant wave height (*Hs*), mean wave period and mean wave direction. A single spatially averaged value for each parameter is returned for each RC at 10 min intervals. The processed data is monitored by Qualitas (2015) and NUIG. Fig. 2 shows the CODAR system in Galway Bay

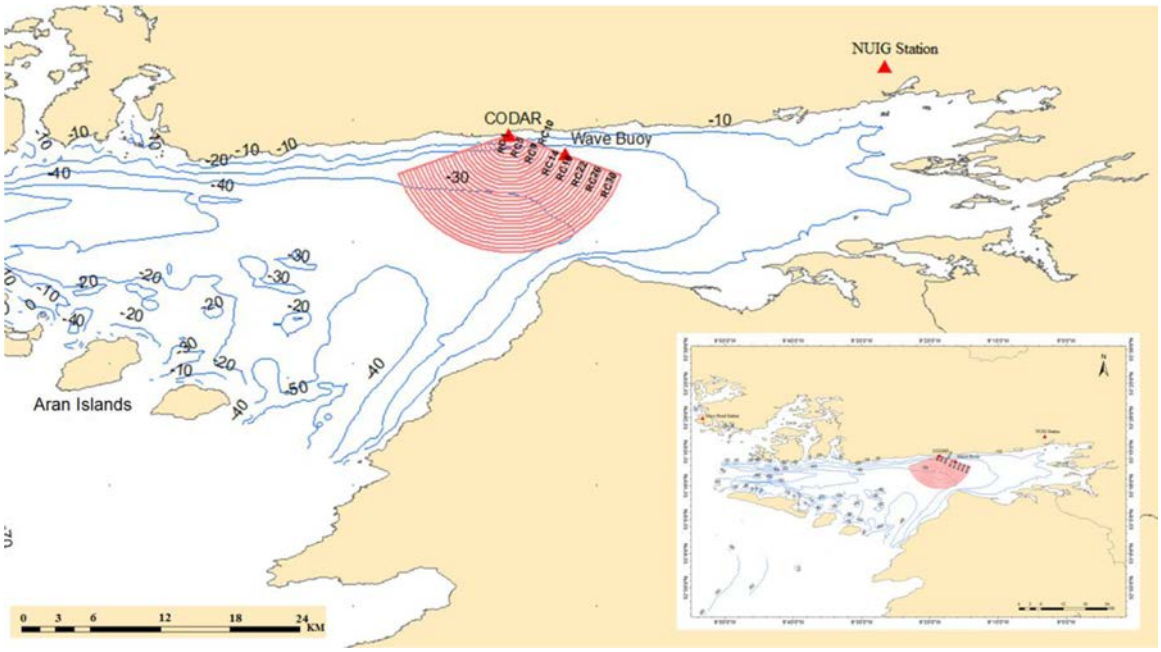

Fig. 2. An overview of the study area and available data locations with 30 RCs for CODAR system in Galway Bay.

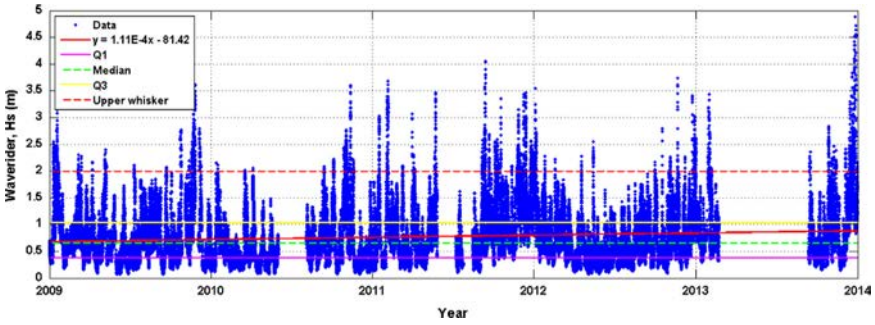

Fig. 3. An overview of available significant wave height, *Hs* (m) data at Spiddal waverider buoy.

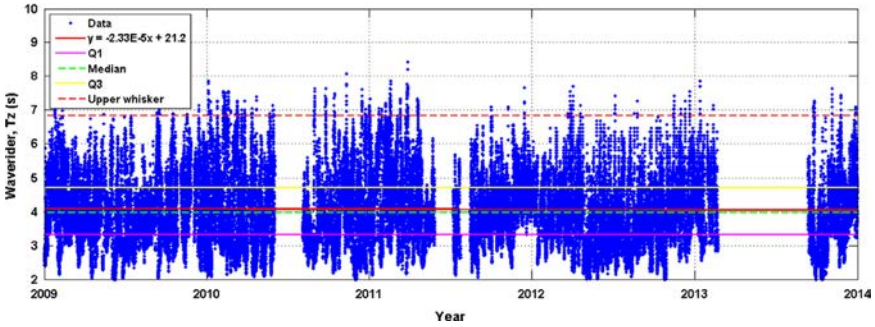

Fig. 4. An overview of available zero-crossing wave period, *Tz* (s) data at Spiddal waverider buoy.

with 30RCs of the Spiddal mast covering the coastline sector between 95° and 263° clockwise from North. The antenna resolution for wave measurement covers a buffer zone of 9 km. CODAR broadcasts radio waves across the ocean surface within the buffer zone. The radio waves are scattered and analysis of Doppler-shifted echoes enables measurement of sea surface conditions. A detailed description of the operating system is discussed in Belinda and Nyden (2005).

The waverider buoy at the wave energy test site (53.227N, −9.271W) is located approximately 4 km from the Spiddal radar mast in waters of approximately 22 m depth. The test site and waverider buoy are monitored and controlled by the Marine Institute (MI). The data is processed from raw spectral files before it can be distributed to another party for further analysis or other purpose. The processed data is supplied by MI through an online data portal, at 30 min time resolution (Marine Institute, 2015).

The assessment methodology used in this paper is detailed as follows:

- Investigation of measured wave data at the 1/4-scale test site during the periods of January 2009–December 2013 for waverider buoy and October to December 2011, January to December 2012, January to February 2013 and September to December 2013 for CODAR.
- A general analysis of wave characteristics at the site, i.e.

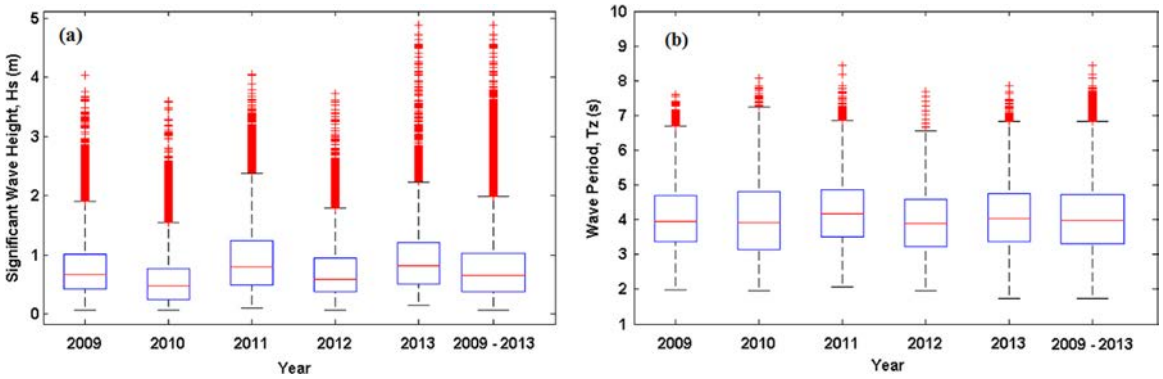

Fig. 5. Box plots of wave data at Spiddal waverider buoy for the year of 2009–2013 and the total of 5 years period: (a) *Hs* and (b) *Tz*.

Table 1
Summary of yearly dataset for *Hs* and *Tz* (2009–2013).

	Hs (m)					*Tz* (s)					Data captured	
Year	Q1	Med	Mean	IQR	UW	Q1	Med	Mean	IQR	UW	Number	%
2009	0.4	0.7	0.8	0.6	1.9	3.4	3.9	4.0	1.3	6.7	15,573	89
2010	0.2	0.5	0.6	0.5	1.6	3.2	3.9	4.1	1.6	7.3	13,776	79
2011	0.5	0.8	0.9	0.8	2.4	3.5	4.2	4.2	1.3	6.9	14,477	83
2012	0.4	0.6	0.7	0.6	1.8	3.2	3.9	4.0	1.4	6.7	17,071	97
2013	0.4	0.7	0.9	0.7	2.0	3.4	3.9	4.1	1.4	6.8	8115	46
2009-2013	0.4	0.6	0.8	0.6	2.0	3.3	4.0	4.1	1.4	6.8	69,012	79

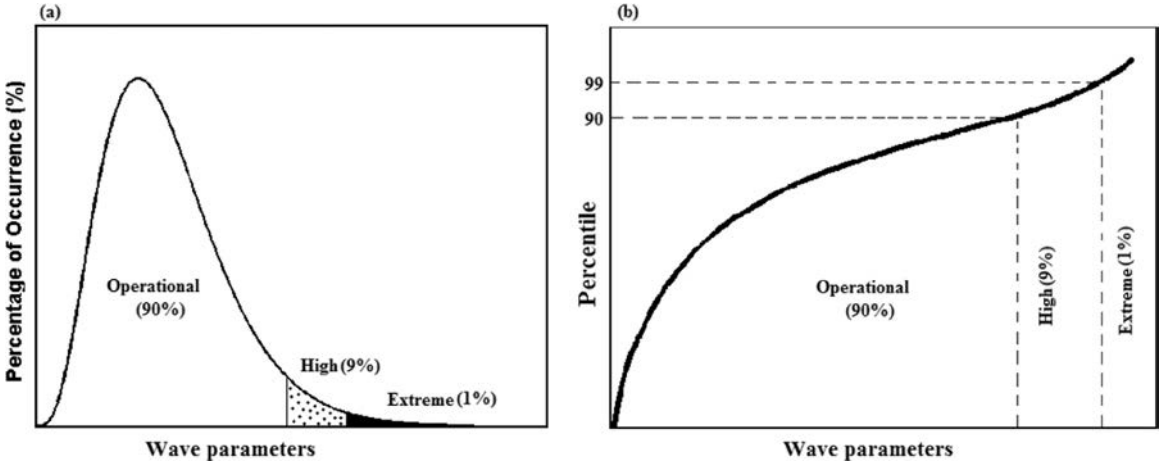

Fig. 6. Graphical representation of site characterisation approach using (a) percentage of occurrences and (b) normalised wave parameters with percentiles.

Table 2
Overview of selected period of yearly and seasonal analysis.

Analysis	Period selection
Yearly	January to December of current year
Winter	December (previous year), January and February (current year). For example, winter 2013 comprises December 2012 to January and February 2013.
Spring	March, April and May of current year
Summer	June, July and August of current year
Autumn	September, October and November of current year

Table 3
Overview of selected period of yearly and seasonal analysis.

Characterisation period	**Operational**	**High**	**Extreme**
2009–2013	$0 > Hs \leq 1.5$	$1.5 < Hs \leq 2.5$	$Hs > 2.5$
2009	$0 > Hs \leq 1.5$	$1.5 < Hs \leq 2.4$	$Hs > 2.4$
2010	$0 > Hs \leq 1.2$	$1.2 < Hs \leq 2.1$	$Hs > 2.1$
2011	$0 > Hs \leq 1.7$	$1.7 < Hs \leq 2.8$	$Hs > 2.8$
2012	$0 > Hs \leq 1.3$	$1.3 < Hs \leq 2.2$	$Hs > 2.2$
2013	$0 > Hs \leq 1.7$	$1.7 < Hs \leq 3.1$	$Hs > 3.1$

significant wave height (*Hs*) and zero-crossing wave period (*Tz*) using waverider buoy data, involves linear time series regression and boxplots analysis; this allows assessment of operational, high and extreme wave events for yearly and seasonal periods

- A more detailed characterisation of the site where annual and seasonal % occurrences of particular events are analysed to identify operational, high and extreme events. The site is characterised firstly by wave height and secondly by wave power; this allows for a comprehensive assessment of wave characteristics and resource variability in Galway Bay.
- Identification of an appropriate outliers condition and suitable RCs for CODAR data to enable calculation of average *Hs* values to be

compared with waverider buoy data for validation purposes. The methodology for outliers and RC selection has been developed based on a preliminary CODAR data assessment (Atan et al., 2014) and an overview is presented in Section 4.1.

- Assessment of accuracy of CODAR data relative to waverider buoy data for wave height characteristics by statistical measures including root mean square error (RMSE), coefficient of determination (R^2) and bias in *Hs* for the selected seasonal periods.
- Detailed analysis of wave heights (using both data sources) based on QQ plots presented for the selected seasonal periods.
- Analysis of CODAR data with respect to available measured wind data at the study area to determine the influence and relationship between wind parameters and *Hs*.

3. Assessment of Waverider data

An assessment of wave characteristics in Galway Bay was conducted based on the Spiddal Waverider buoy data January 2009–December 2013 at 30 min interval. An overview of significant wave height (*Hs*) and zero-crossing wave period (*Tz*) characteristics at the site is presented. In addition, the site is characterised based on both wave height and wave power using a methodology for site characterisation based on percentage of wave occurrences and normalised wave power parameters developed by the authors.

3.1. Wave height and wave period characteristics

Figs. 3 and 4 show the variation of *Hs* and *Tz*, respectively, as measured by the waverider at the site for the period of January

Table 4
Summary of yearly wave conditions based on wave power, *P*.

Characterisation period	Operational	High	Extreme
2009–2013	$0 > P \leq 7$	$7 < P \leq 25$	$P > 25$
2009	$0 > P \leq 7$	$7 < P \leq 21$	$P > 21$
2010	$0 > P \leq 5$	$5 < P \leq 15$	$P > 15$
2011	$0 > P \leq 10$	$10 < P \leq 32$	$P > 32$
2012	$0 > P \leq 5$	$5 < P \leq 18$	$P > 18$
2013	$0 > P \leq 10$	$10 < P \leq 40$	$P > 40$

Table 5
Summary of seasonal wave conditions based on wave power.

Characterisation period	Operational	High	Extreme
Winter 2009	$0 > P \leq 8$	$8 < P \leq 22$	$P > 22$
Winter 2010	$0 > P \leq 4$	$4 < P \leq 15$	$P > 15$
Winter 2011	$0 > P \leq 6$	$6 < P \leq 37$	$P > 37$
Winter 2012	$0 > P \leq 12$	$12 < P \leq 31$	$P > 31$
Winter 2013	$0 > P \leq 10$	$10 < P \leq 29$	$P > 29$
Spring 2009	$0 > P \leq 6$	$6 < P \leq 17$	$P > 17$
Spring 2010	$0 > P \leq 3$	$3 < P \leq 10$	$P > 10$
Spring 2011	$0 > P \leq 6$	$6 < P \leq 18$	$P > 18$
Spring 2012	$0 > P \leq 4$	$4 < P \leq 10$	$P > 10$
Summer 2009	$0 > P \leq 5$	$5 < P \leq 11$	$P > 11$
Summer 2010	$0 > P \leq 2$	$2 < P \leq 4$	$P > 4$
Summer 2011	$0 > P \leq 2$	$2 < P \leq 6$	$P > 6$
Summer 2012	$0 > P \leq 3$	$3 < P \leq 6$	$P > 6$
Autumn 2009	$0 > P \leq 9$	$9 < P \leq 32$	$P > 32$
Autumn 2010	$0 > P \leq 7$	$7 < P \leq 17$	$P > 17$
Autumn 2011	$0 > P \leq 12$	$12 < P \leq 28$	$P > 28$
Autumn 2012	$0 > P \leq 6$	$6 < P \leq 13$	$P > 13$
Autumn 2013	$0 > P \leq 6$	$6 < P \leq 18$	$P > 18$

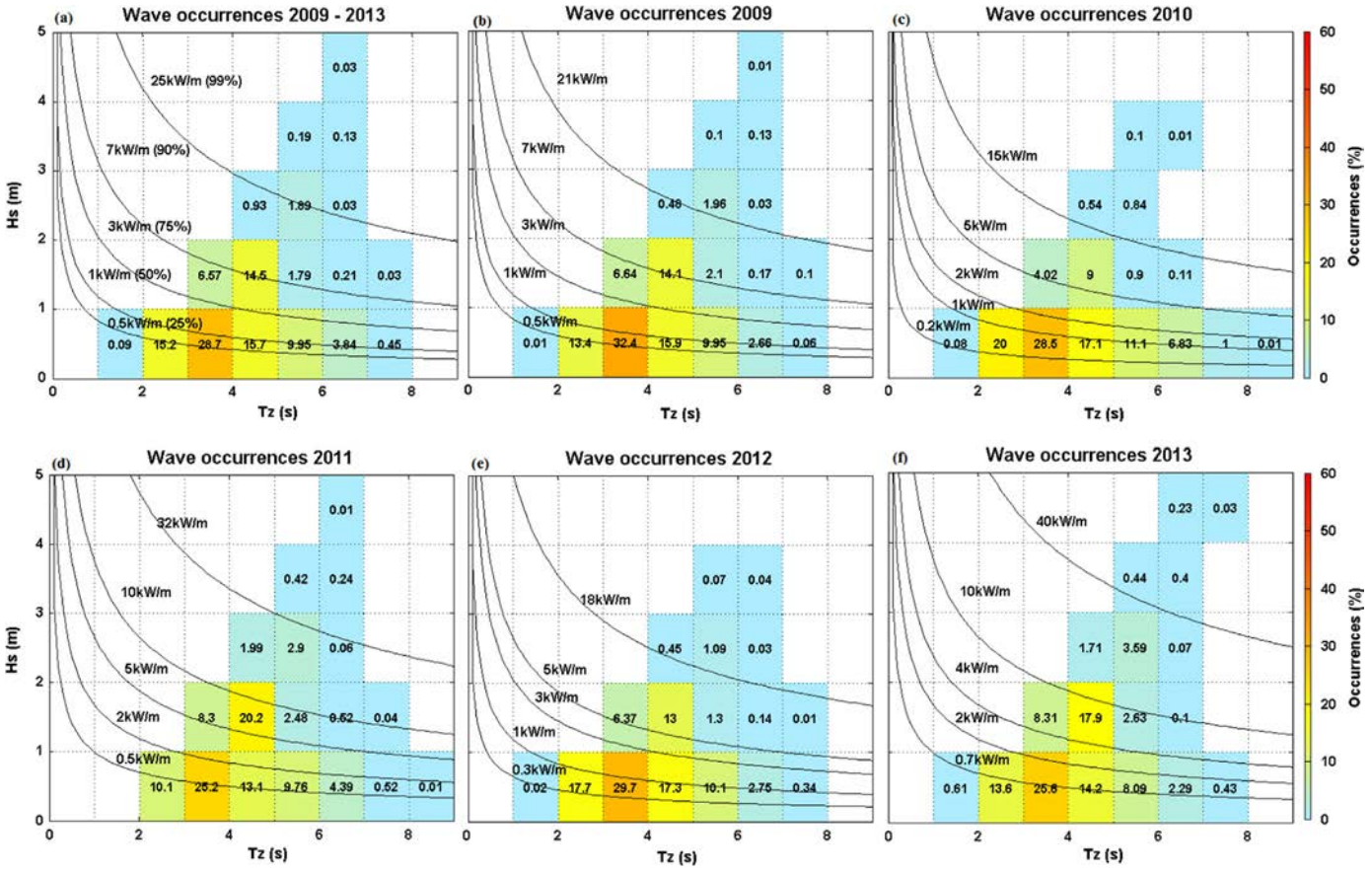

Fig. 7. Percentage of wave occurrences between significant wave height, *Hs* (m), and zero up-crossing wave period, *Tz* (s), with wave power isolines for (a) 2009-2013, (b) 2009, (c) 2010, (d) 2011, (e) 2012, (f) 2013.

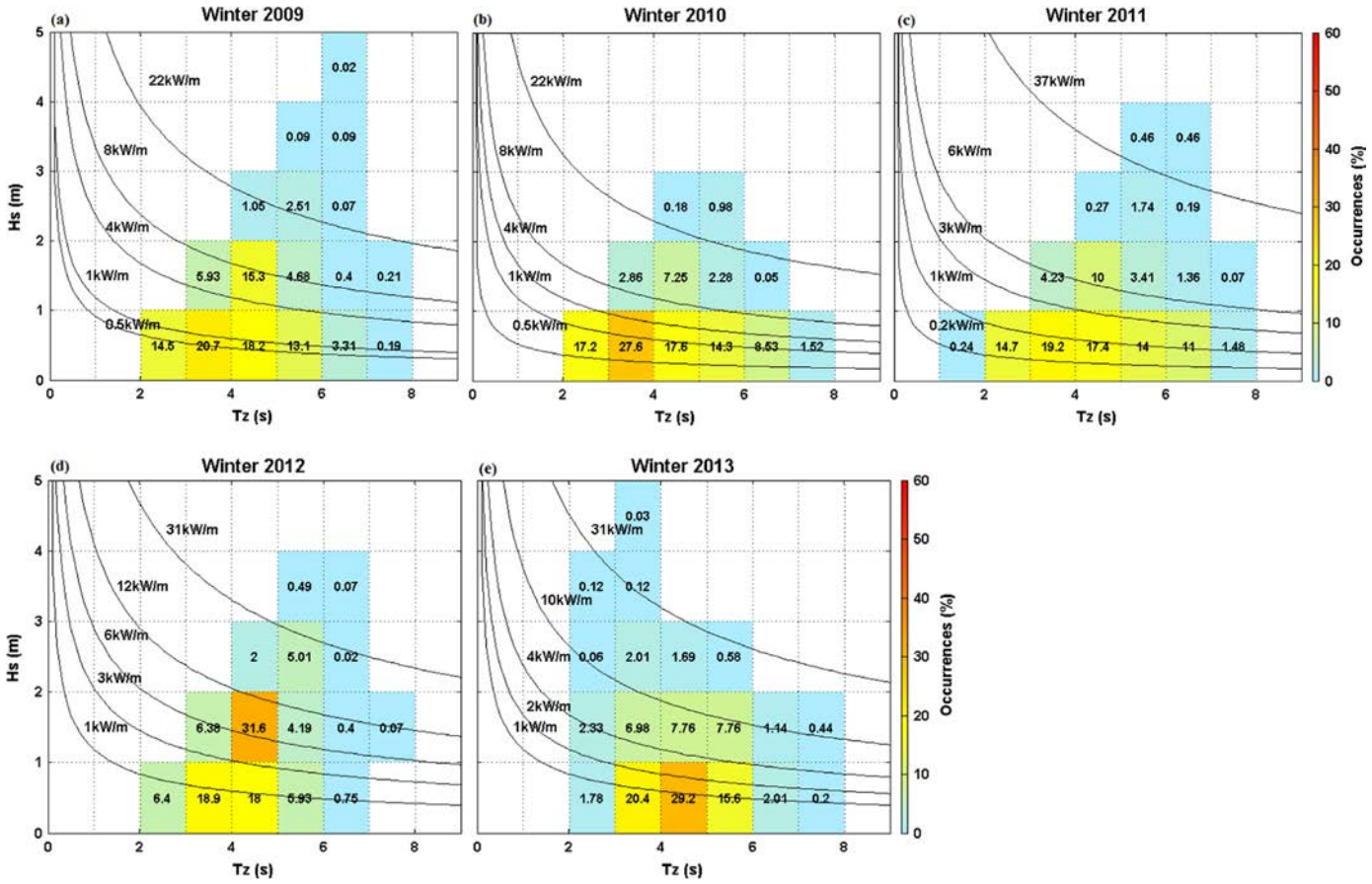

Fig. 8. Percentage of wave occurrences between significant wave height, *Hs* (m) and zero up-crossing wave period, *Tz* with wave power isolines for winter periods (a) 2009, (b) 2010, (c) 2011, (d) 2012 and (e) 2013.

2009–December 2013. The figures show that gaps are present in the dataset (due to instrument downtime), most notably for the summer periods in 2010, 2011 and 2013. The impacts of these gaps on the wave characteristics assessment are discussed later. A linear time series regression and equation are shown in Figs. 3 and 4, along with the 25th quantile (Q1), median and 75th quantile (Q3) lines and an upper whisker line which can be calculated based on Q3 and the inter quantile range (IQR) as:

$$\text{Upper whisker} = \text{Q3} + 1.5\text{IQR} \quad (1)$$

It can be seen from the figures that the mean *Hs* and *Tz* at the site for the 5-year period are 0.8 m and 4.1 s respectively. As would be expected, a general trend of higher waves in winter and smaller waves in summer is present in Fig. 3.

The inter-annual variation in *Hs* and *Tz* characteristics was further investigated using box plot analyses. An overview of the dataset trends is shown in yearly boxplots of *Hs* and *Tz* (Fig. 5) where Q1, median, Q3 and upper whisker (UW) can be interpreted for each year; a summary of these values are tabulated in Table 1. From Table 1, it can be seen that the annual mean values of *Hs* vary from 0.6 to 0.9 m. The highest wave events can be seen to have occurred in 2013, while in 2010 wave heights were lower than average. The maximum *Hs* during the period was 4.9 m in 2013 and resulted from a high wind speed event in winter 2013 with wind speeds of up to 35 m/s recorded at the Mace Head meteorological station, located on the Atlantic coast west of Galway Bay. Annual mean values of *Hs* are quite consistent and vary from 4 to 4.2 s. The longest *Tz* of up to 8.5 s in 2011 is due to long swell waves from AO entering Galway Bay.

3.2. Site characterisation

Characterising the wave climate at a site typically involves ascertaining the operational, i.e. average, and extreme wave events at the site. With regards to wave energy devices, knowing the operational conditions is important for energy capture as the device should be designed to extract power most efficiently in those conditions as they occur most often. However, knowing the extreme conditions is also important with regards to survivability of the device. In the absence of any defined methodology and/or criteria in the literature for defining operational and extreme wave conditions at a site, we developed our own methodology and criteria. The methodology is based on percentage of wave occurrences with criteria for operational, high and extreme conditions defined as percentiles of normalised wave parameter data. The approach is generic and can be applied to any site and any wave parameter, γ, once measured data is available. This means that one can characterise a site separately by wave height, wave period or wave power.

Fig. 6 shows a graphical representation of the characterisation methodology using both a percentage occurrence plot and a normalised wave parameters plot with percentiles. The characterisation of a site by wave parameter, γ, is conducted simply by graphing the normalised wave parameter data (Fig. 6b) and applying the following criteria:

- Operational events:events falling between 0th and 90th percentiles.
- High events:events falling between 90th and 99th percentiles.
- Extreme events:events falling between 99th and 100th percentiles.

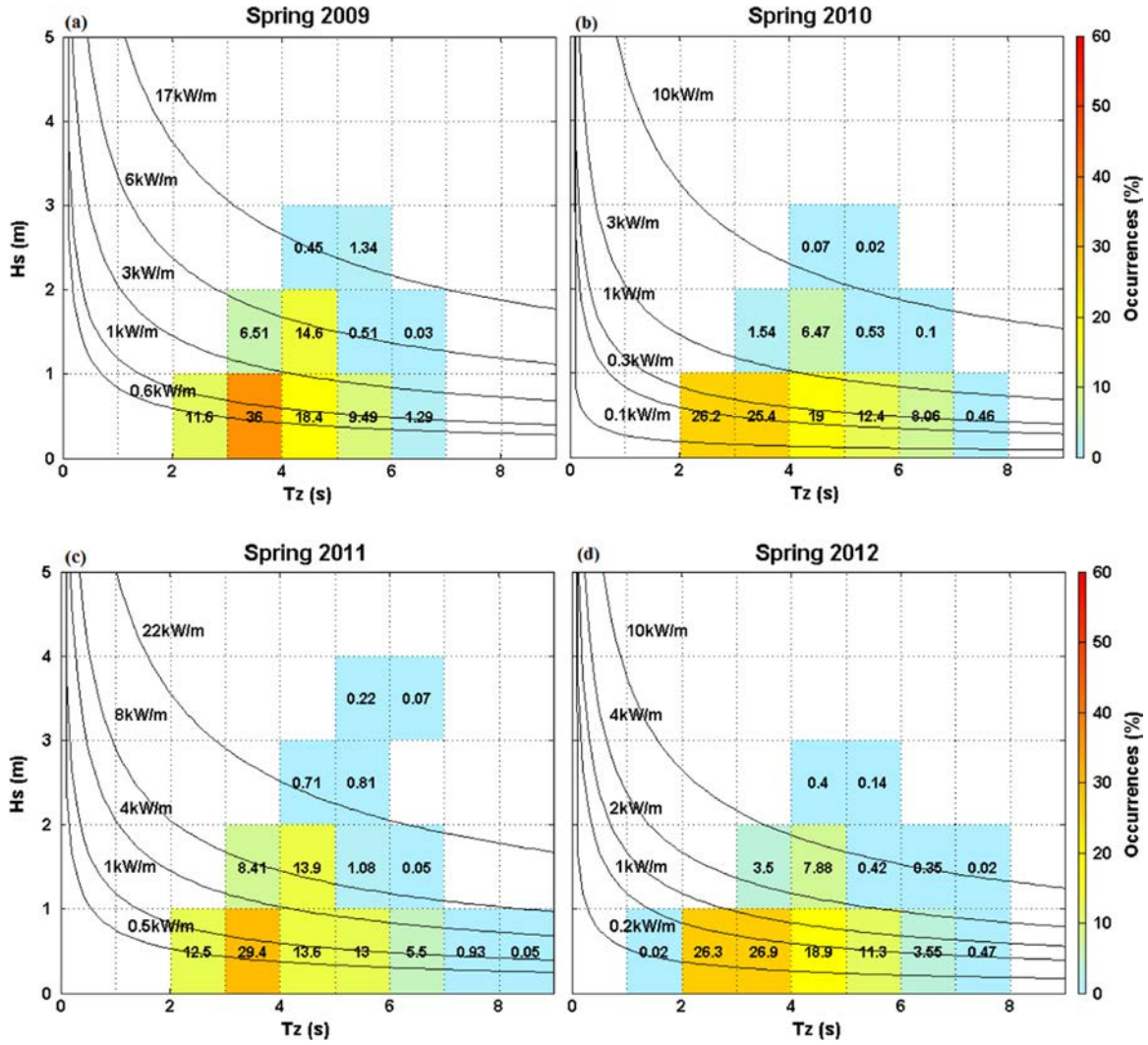

Fig. 9. Percentage of wave occurrences between significant wave height, *Hs* (m) and zero up-crossing wave period, *Tz* with wave power isolines for spring periods (a) 2009, (b) 2010, (c) 2011 and (d) 2012.

The characterisation methodology was applied to the Galway Bay, 1/4 scale test site to identify operational, high and extreme wave conditions. Separate characterisations were conducted for significant wave height (*Hs*) and wave power (*P*), as these are important design parameters for device survivability and energy capture, respectively. Yearly and seasonal analysis analyses were conducted using the seasonal periods defined in Table 2. It should be noted from the table that the winter period for a particular year runs from December of the previous year to February of the current year, while the yearly analysis period runs from January to December of each year. Hence, some discrepancies exist between the yearly and seasonal analyses results.

3.2.1. Characterisation based on significant wave height

Significant wave height (*Hs*) characteristics at the site were identified based on the approach presented in the previous section. Characterisations were performed for the full 5-year period and for each individual year. For the 5-year period, the upper threshold of operational *Hs* was 1.5 m, while the lower threshold of extreme *Hs* was 2.5 m. Comparing the annual characteristics, it is seen that there was an inter-annual variation of 0.5 m in the upper threshold of operational *Hs* and of 1 m in the lower threshold of extreme *Hs* events. 2011 and 2013 wave climates were more energetic compared to the other years with operational *Hs* thresholds of 1.7 m compared to the 5-year value of 1.5 m and extreme *Hs* thresholds of 2.8 m and 3.1 m, respectively, compared to the 5-year value of 2.5 m. It should be noted, however, that the 2013 analysis only included winter and autumn data due to the non-availability of spring and summer data. The lowest operational and extreme *Hs* thresholds of 1.2 m and 2.1 m occurred in 2010 and indicate that 2010s wave climate was less energetic than normal. The *Hs* characteristics presented in Table 3 provide important information for wave energy device designers in relation to the survivability of their scaled prototypes at the 1/4 scale test site. In Section 4, a similar characterisation is perform using high frequency radar (i.e. CODAR) data to determine their accuracy.

As previously stated, data from the waverider were not available for parts of the summer periods in 2010, 2011 and 2013. Given that mean wave heights in summer are lower than those in spring, autumn and winter, the likely impact of the summer data gaps on the yearly analyses is that the threshold wave heights for 2010, 2011 and 2013 presented in Table 3 would likely be slightly lower were the missing data included in the analyses.

3.2.2. Characterisation based on wave power

The power extracted by a wave energy device is directly proportional to the power available to it; a good understanding of the power available at a site is therefore crucial. The power per unit

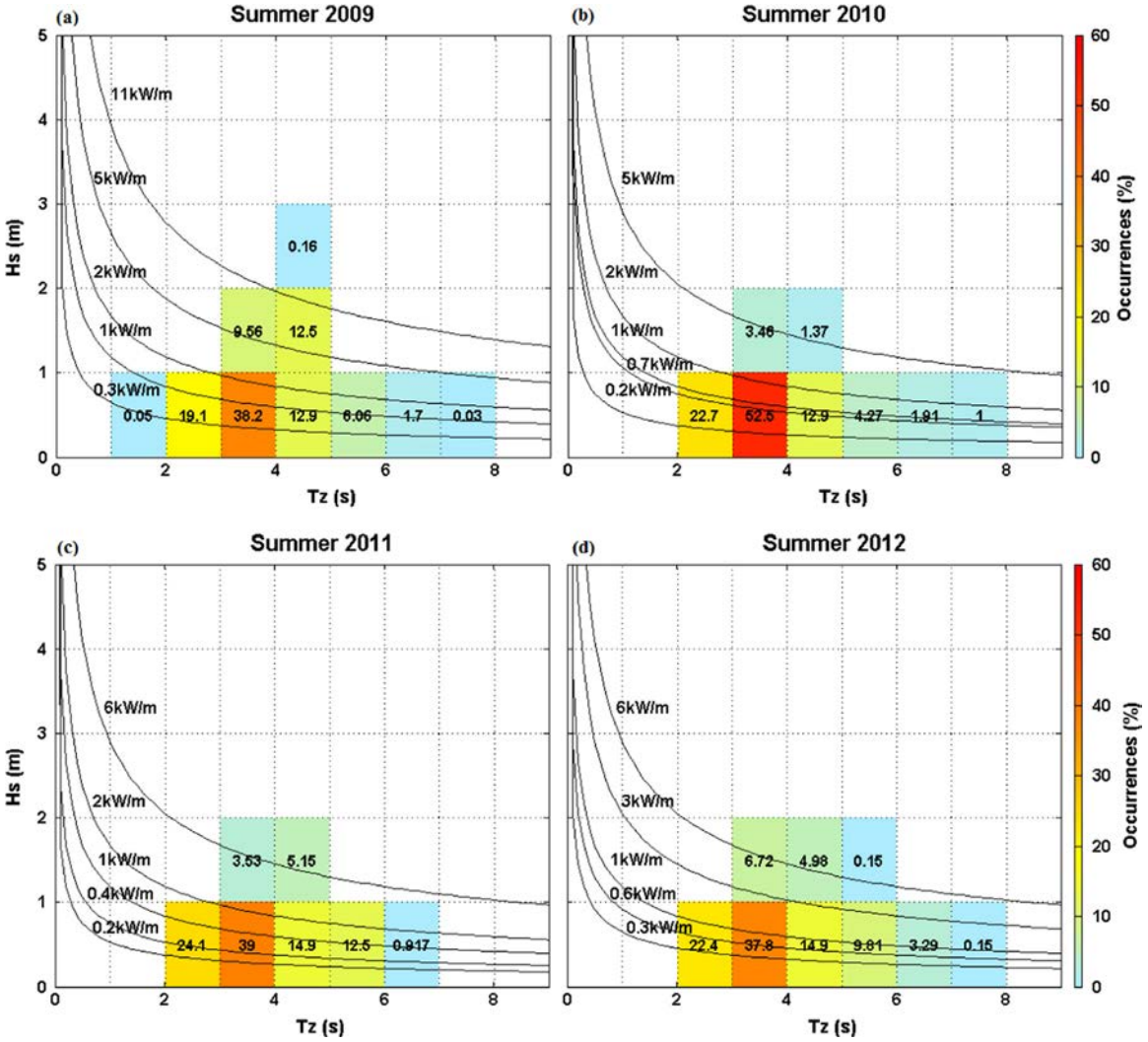

Fig. 10. Percentage of wave occurrences between significant wave height, *Hs* (m) and zero up-crossing wave period, *Tz* with wave power isolines for summer periods (a) 2009, (b) 2010, (c) 2011 and (d) 2012.

width of wave crest (kW/m) of a regular sea state deep water wave can be calculated using Eq. (2), where *Te* is the wave energy period. A specific wave period ratio between *Te* and *Tz* (*Te*/*Tz*) should be applied in order to avoid underestimation of wave power. (Cahill, 2013) presents a comprehensive explanation of wave period ratios in Ireland and specifically at the two wave energy test sites - AMETS and Galway Bay. The wave period ratio of 1.447 determined by Cahill (2013) for the Galway Bay test site is used here.

Eq. (2) was used, along with *Hs* and *Tz* data, to calculate estimates of available wave power in Galway Bay. The authors' characterisation methodology was then applied to the wave power data to obtain threshold values for operational, high and extreme wave power events. Once again, separate characterisations were performed for the full 5-year period and for each individual year. The results of the wave power characterisation are summarised in Table 4.

$$P = 0.49Hs2Te = 0.71Hs2Tz \quad (2)$$

From Table 4, it can be seen that the upper threshold of operational *P* events for the 5 year period 2009–2013 was 7 kW/m but this varied annually from 5 to 10 kW/m. The lower threshold of extreme *P* events was 25 kW/m for the 5-year period and varied annually from 15 to 40 kW/m. As with the characterisation by wave height, the results of the characterisation by wave power indicate that the wave climate at the site was more energetic than normal in 2011 and 2013 and less energetic than normal in 2010 with higher operational and extreme threshold values recorded in 2011 and 2013 compared to the 5-year values and lower threshold values recorded in 2010.

Fig. 7 presents the results of the characterisation analysis by overlaying the 90th (upper operational threshold) and 99th (lower extreme event threshold) wave power percentile isolines on joint occurrence plots of *Hs* and *Tz*. For additional information the 25th, 50th and 75th wave power percentile isolines are also included. These plots give a useful indication of the ranges of heights and periods of the waves that comprise operational and extreme wave power events. Furthermore, they also allow one to determine the ranges of heights and periods that represent the majority of operational, high or extreme wave power events. It is observed that for operational waves *Hs* can range from 0 to 2 m and *Tz* can range from 1 to 9 s, but the most common operational wave conditions year on year have *Hs* of between 0 and 1 m and *Tz* between 2 and 6 s; such waves account for more than 50% of the wave conditions at the site annually. Typical high wave events at the site have *Hs* of between 1 and 3.2 m and *Tz* between 4 and 8 s, while extreme wave events typically have Hs between 2 and 5 m and *Tz* between 4 and 7 s. The plots corroborate the earlier indications that 2011 and 2013 had more energetic wave climates than normal, and that

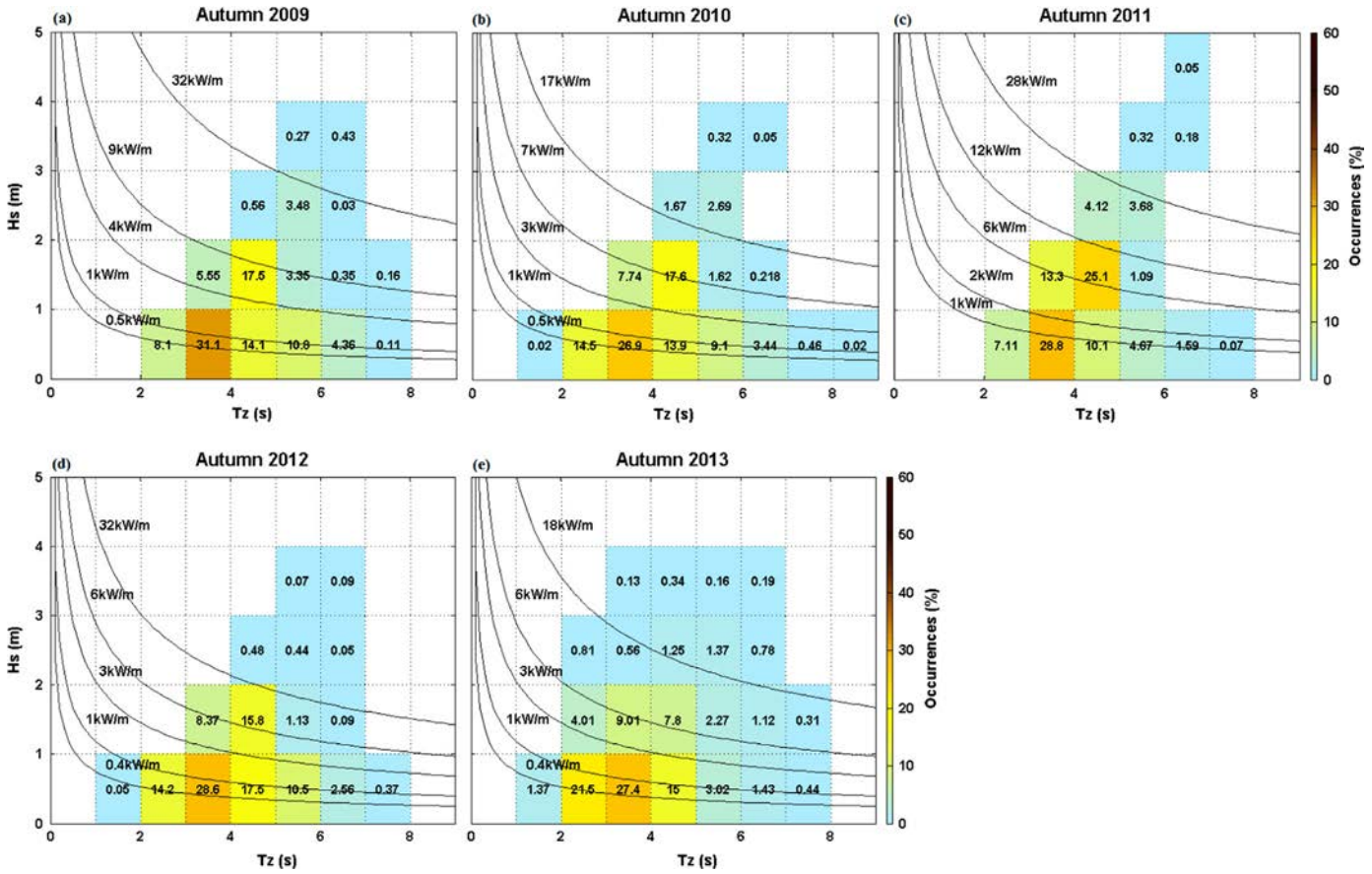

Fig. 11. Percentage of wave occurrences between significant wave height, *Hs* (m) and zero up-crossing wave period, *Tz* with wave power isolines for autumn periods (a) 2009, (b) 2010, (c) 2011, (d) 2012 and (e) 2013.

Table 6
Summary of yearly and seasonal wave power estimation (kW/m). NA indicates non-available data.

Year	Yearly			Winter			Spring			Summer			Autumn		
	Mean	± SD	Max	Mean	± SD	Max	Mean	± SD	Max	Mean	± SD	Max	Mean	± SD	Max
2009	2.7	± 4.4	73.5	3.3	± 5.0	73.5	2.4	± 3.0	20.4	1.8	± 2.3	15.7	3.6	± 6.2	57.2
2010	1.7	± 3.3	31.9	1.6	± 2.9	31.9	1.0	± 1.8	15.5	1.0	± 0.9	5.7	2.7	± 3.6	27.6
2011	3.9	± 6.0	75.4	2.8	± 6.0	64.5	2.4	± 4.1	52.1	0.9	± 1.2	8.9	4.9	± 6.3	75.4
2012	2.2	± 3.6	63.7	5.1	± 3.6	53.5	1.3	± 2.1	23.4	1.1	± 1.4	10.6	2.4	± 3.6	63.7
2013	4.2	± 8.1	50.8	4.0	± 5.6	50.8	NA	NA	NA	NA	NA	NA	2.3	± 3.5	31.2
2009 –2013	2.8	± 5.1	75.4	3.3	± 5.1	73.5	2.0	± 2.8	52.1	1.2	± 1.4	15.7	3.2	± 4.7	75.4

2010 had a less energetic climate than normal. The inclusion of the 25th, 50th and 75th wave power percentile isolines can provide very useful information to developers when considering the proportion of available power to target versus the cost of designing a device that is able to operate and survive the sea-states that prevail during those wave power conditions.

To investigate seasonal wave power conditions, the authors' methodology was used to conduct seasonal wave power characterisations for winter, spring summer and autumn as defined in Table 2. Due to limited data, Spring 2013 and Summer 2013 were omitted from the analysis. A summary of the seasonal characterisations for each year is presented in Table 5. It can be seen that there is significant variability in wave power conditions at the test site between seasons. The highest operational and extreme waves occur in autumn and winter and the lowest occur in summer. Taking 2012 as an example the winter operational threshold was 12 kW/m compared to just 3 kW/m in summer. This demonstrates the need to conduct seasonal site characterisations when considering deployment of test devices. The seasonal analyses also provide additional context to the annual analyses. For example, the annual analyses indicated that 2011 had one of the most energetic wave climates of the 5-year period and that 2010 had the least energetic; however, when we look at the winter seasonal characteristics, we see that the operational P threshold for 2011 (6 kW/m) was the second lowest of the 5 years. By contrast, the autumn characteristics show that the 2011 operational P threshold (12 kW/m) was significantly higher than that for the other years. Thus, 2011 did not have more energetic waves than other years throughout the whole course of the year, but rather its autumn waves were significantly more energetic than those of other years.

To determine the impacts of the summer data gaps on the summer wave power characterisations, a wave model of Irish coastal waters (Atan, Goggins and Nash, 2015) resolved at 0.05 degrees was used to simulate the summer periods of 2010 and 2011 and the model results used to perform summer wave power characterisations to compare with those presented in Table 5.

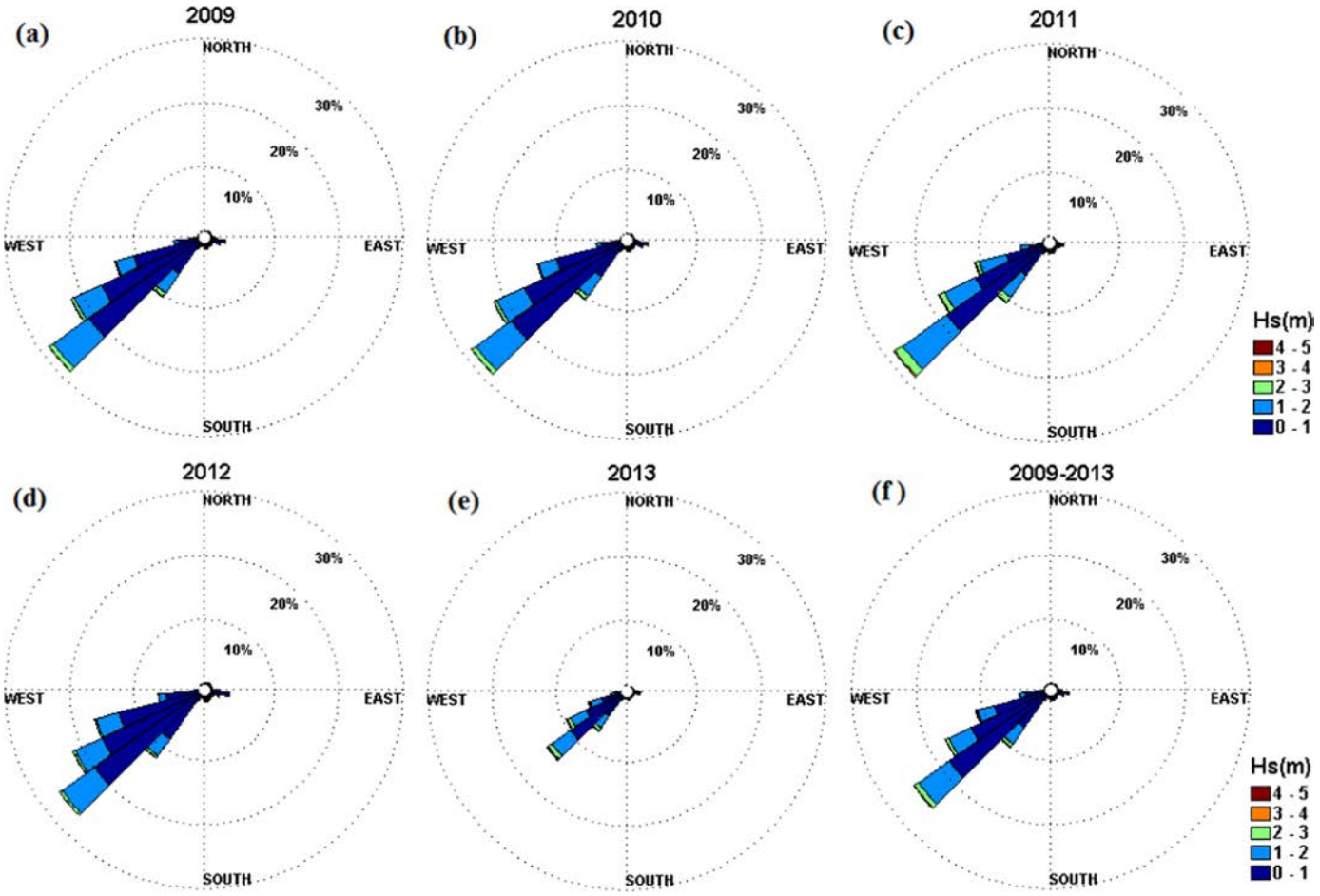

Fig. 12. Yearly wave roses from 2009 to 2013. (a) 2009, (b) 2010, (c) 2011, (d) 2012, (e) 2013 and (f) 2009–2013.

Table 7
Percentage of captured data for CODAR *Hs* (December 2012).

RC	Percentage of captured data	RC	Percentage of captured data	RC	Percentage of captured data
1	0	11	78	21	87
2	0.1	12	82	22	87
3	0.1	13	85	23	87
4	5	14	86	24	86
5	13	15	87	25	85
6	19	16	87	26	85
7	32	17	87	27	85
8	50	18	88	28	85
9	64	19	87	29	85
10	73	20	88	30	84

Model accuracy for summer conditions was first determined by comparing model results with measured data from August 2010 and 2011. RMSE, R^2 and bias values for modelled H_s were calculated as 0.17 m, 0.81 and 0.23 m, respectively, for August 2010 and 0.18 m, 0.88 and 0.2 m, respectively, for August 2011. These values confirm the model can accurately reproduce summer wave climates.

The characterisation using model outputs gave operational thresholds of 6 kW/m and 5 kW/m in Summer 2010 and 2011, respectively. These are higher than the 2 kW/m thresholds calculated using the measured data (Table 5), but are similar in magnitude to the 5 kW/m threshold calculated for the full set of summer data in 2009. This suggests that the typical summer operational wave power threshold is of the order of 5 kW/m. The

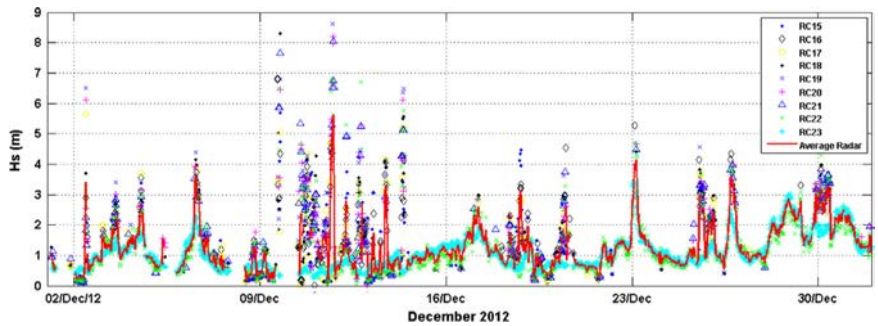

Fig. 13. Comparison of *Hs* for individual range cells with highest percentage of captured data (RC 15–23 in Table 1) against *Hs* averaged values in December 2012.

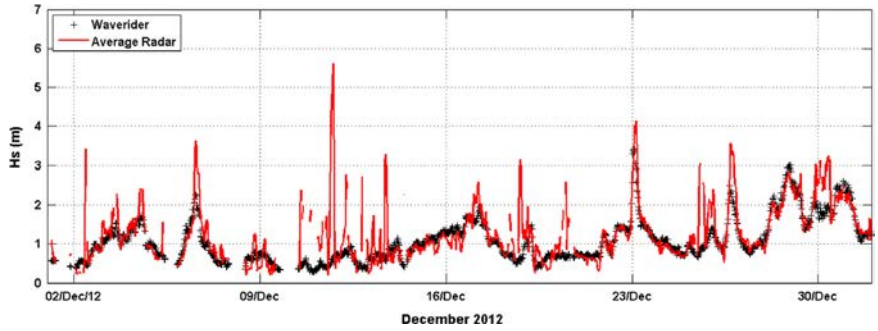

Fig. 14. Comparison of *Hs* waverider buoy against CODAR averaged values in December 2012.

characterisation using model outputs also gave an extreme threshold of 14 kW/m for both summer periods in 2010 and 2011. This compared with extreme thresholds of 5 kW/m and 6 kW/m for 2010 and 2011, respectively, when using the available measured data. The higher extreme thresholds from the model outputs characterisation are again more in line with the extreme threshold of 11 kW/m calculated for summer 2009 from a full set of measured data, suggesting that the typical summer extreme wave power threshold is of this order of magnitude. The results of the data gap analyses highlight the importance of high temporal coverage of data for accurate site characterisations. From Table 5, it can be seen that, for the Galway Bay site, the summer period is the least energetic period of the year with Winter extreme thresholds of the order of 20–30 kW/m. Winter conditions are therefore more important in terms of device survival design and the summer data gaps are thus considered insignificant from this point of view.

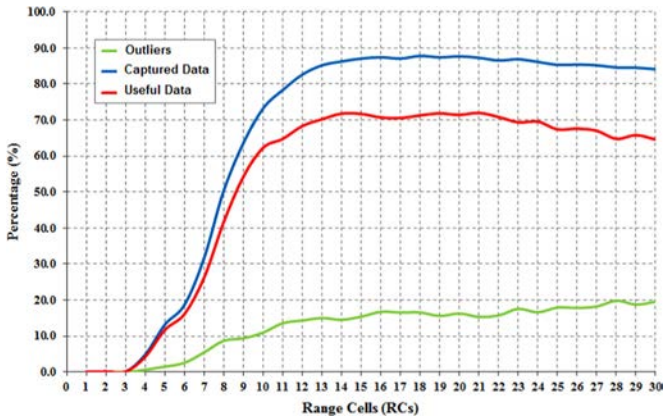

Fig. 15. The overview of useful data for RCs selection at 30 RCs for December 2012 based on outliers 50%.

Figs. 8–11 show joint occurrence plots for *Hs* and *Tz* for winter, spring, summer and autumn periods, respectively. The characterisation threshold (90th and 99th percentile) isolines and the 25th, 50th and 75th percentile isolines are also overlaid. With the exception of just two of the seasons analysed - winter 2012 and 2013 - the most frequently occurring waves within the operational power range had $Hs < 1$ m and $3 < Tz < 4$ s. Waves of this type typically contributed 30–40% of operational wave power events. With the exclusion of summer, extreme wave power events typically comprised waves with 2 m $< Hs <$ 5 m and $4 \leq Tz \leq 7$ s. Once again this type of information gleaned from the joint occurrence and wave power isoline plots should be particularly useful for wave energy device developers for optimising performance and engineering for survivability.

In addition to characterising the operational, high and extreme wave power conditions at the site, annual and seasonal mean and maximum available wave powers were determined. These are presented in Table 6; standard deviations are also included. Based on Table 6, it can be seen that while the 5-year mean annual wave power was calculated at 2.8 kW/m; there is significant inter-annual variability with annual means ranging from 2 to 4 kW/m. The winter period shows the highest 5-year seasonal mean wave power at 3.3 kW/m. In contrast, the summer period shows the lowest 5-year seasonal mean at 1.2 kW/m. It is also observed that autumn 2011 and winter 2012 were particularly energetic compared to other seasons and that the 2013 annual mean is skewed due to the absence of spring and summer data. Wave direction was also analysed through wave rose plots; these are shown in Fig. 12. It is clear that the dominant wave direction is from the south west sector due to the prevailing south-westerly winds on the west coast of Ireland. A detailed assessment of the wind climate in Galway Bay is presented in Section 4.5.

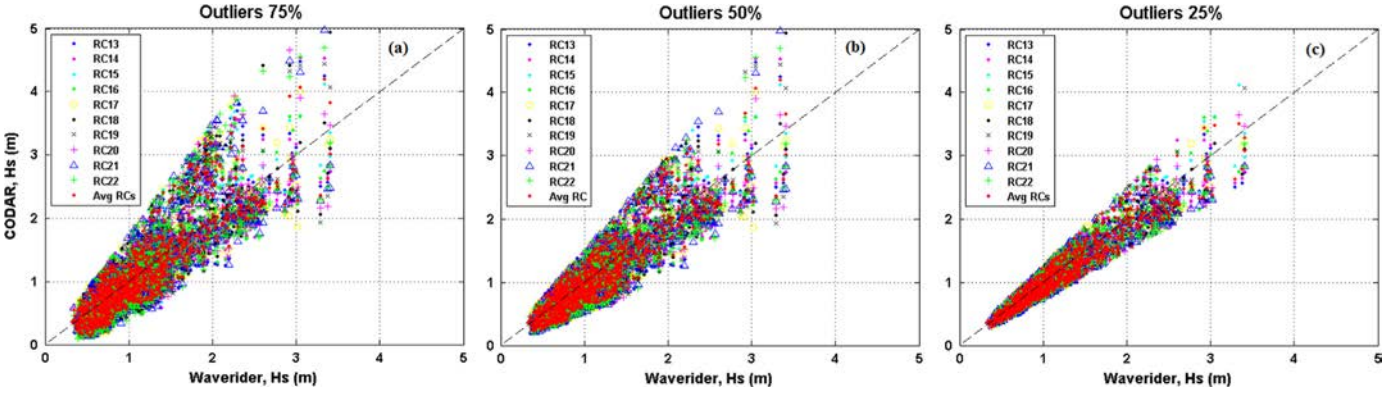

Fig. 16. Scatter plot of useful data from outliers and RCs for December 2012 (a) outliers 75% (b) outliers 50% (c) outliers 25%.

Table 8
Summary of comparative analysis for outliers 75%, 50% and 25%.

RC	Outlier 75%				Outlier 50%				Outlier 25%			
	RMSE	R^2	Bias	Data counts	RMSE	R^2	Bias	Data counts	RMSE	R^2	Bias	Data counts
13	0.3	0.74	0.07	1139	0.3	0.79	0.10	1045	0.2	0.91	0.08	677
14	0.3	0.75	0.06	1163	0.3	0.79	0.08	1068	0.2	0.90	0.06	716
15	0.3	0.76	0.04	1176	0.3	0.82	0.06	1067	0.2	0.91	0.05	755
16	0.3	0.75	0.04	1167	0.3	0.80	0.07	1052	0.2	0.91	0.06	722
17	0.3	0.73	0.04	1166	0.3	0.78	0.07	1050	0.2	0.91	0.07	690
18	0.3	0.73	0.03	1192	0.3	0.78	0.06	1061	0.2	0.91	0.07	726
19	0.3	0.74	0.04	1178	0.3	0.79	0.07	1069	0.2	0.89	0.07	760
20	0.3	0.73	0.04	1187	0.3	0.79	0.08	1071	0.2	0.90	0.06	716
21	0.4	0.72	0.04	1187	0.3	0.77	0.07	1071	0.2	0.90	0.07	716
22	0.4	0.72	0.04	1184	0.3	0.77	0.08	1054	0.2	0.90	0.07	686
Average radar	0.3	0.78	0.03	1286	0.3	0.83	0.05	1258	0.1	0.92	0.06	1085

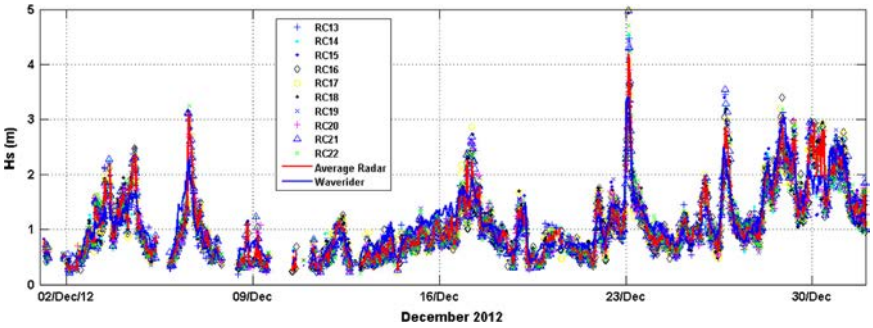

Fig. 17. Comparison of *Hs* for individual range cells (useful data) with *Hs* averaged for a number of selected RCs (13–22) in December 2012.

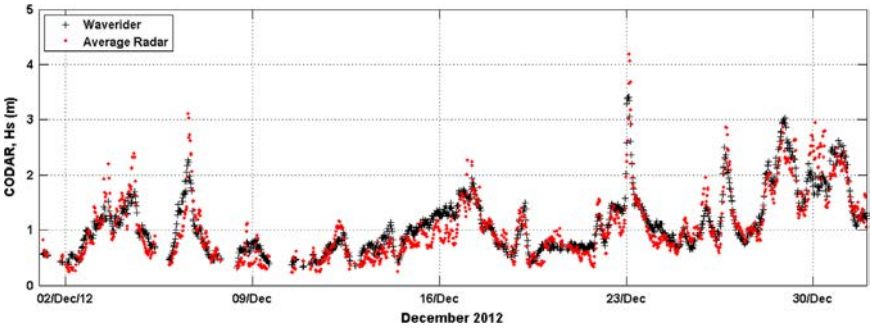

Fig. 18. Comparison of *Hs* waverider buoy against CODAR averaged values in December 2012.

Table 9
Summary of selected RCs for a period of October–December 2013.

Period	Selected RCs	Period	Selected RCs
October 2011	7–10	September 2012	13–19
November 2011	8–14	October 2012	22–30
December 2011	9–14	November 2012	18–25
January 2012	10–18	December 2012	13–22
February 2012	17–22	January 2013	21–25
March 2012	15–22	February 2013	14–23
May 2012	19–22	September 2013	19–25
June 2012	16–21	October 2013	12–14
July 2012	16–23	November 2013	13–15
August 2012	16–24	December 2013	12–14

4. CODAR assessment

CODAR data from the Galway bay radar was available at 10 min intervals from 30 RCs for the 2011 and 2012 periods and from 15 RCs for the 2013 period. As CODAR data is retrieved at individual RCs, an identification process of the RCs to be used in a detailed data assessment was conducted; the details of this process are presented below. The RC selection process also takes consideration of data from the Spiddal waverider buoy, where the data was recorded at 30 min intervals (refer to Fig. 2 for locations). Hence, the CODAR data was subsampled at 30 min interval in order to provide consistency in the temporal resolution of the data for validation and analysis.

4.1. CODAR outliers and range cells (RCs) selection

The capability of CODAR to retrieve incoming signals is dependent on the properties of the sea surface. As a consequence CODAR may or may not be able to successfully record wave properties at a given time. The percentage of captured data may therefore be different for each RC. To demonstrate, Table 7 presents the percentage of captured data for all RCs from RC 1 (0.3 km from CODAR origin) to RC 30 (9 km from CODAR origin) for December 2012.

An initial selection of RC data was to use the data from those RCs with the highest percentage of captured data. From Table 7, for example, RC15–RC23 were selected for the averaging process.

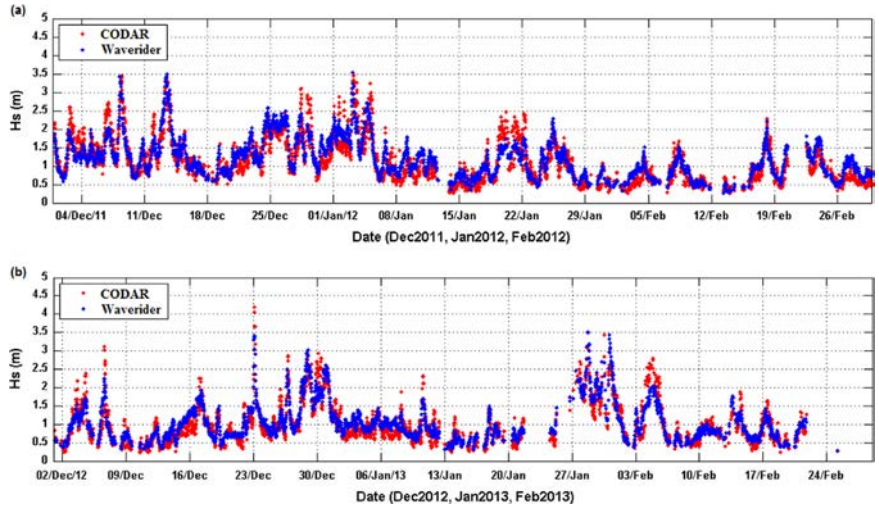

Fig. 19. Comparison of temporal variation of *Hs* between CODAR and wave buoy *Hs* data for Winter (a) 2012 and (b) 2013.

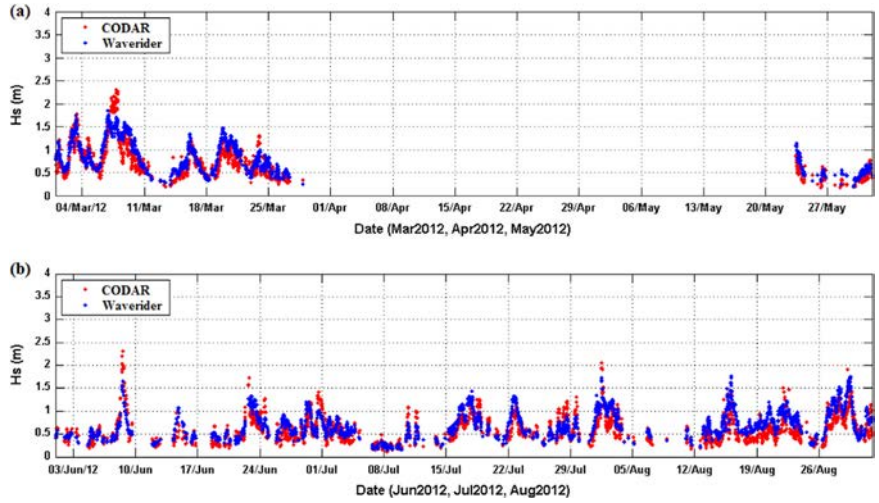

Fig. 20. Comparison of temporal variation of *Hs* between CODAR and wave buoy for (a) spring 2012 and (b) summer 2012.

Fig. 13 shows a comparison plot between *Hs* for each individual RC from RC15 to RC 23 against a spatially-averaged *Hs* calculated from the values for RC15 to RC23. Fig. 14 then compares these spatially-averaged values for *Hs* from CODAR with those obtained from the waverider buoy.

It is clear from Fig. 14 that the initial approach of calculating average values for *Hs* from those RCs with the highest percentage of captured data yields substantially different values to those from waverider buoy data. Hence, it is important to perform some further analysis of the CODAR data before using it for wave characteristic studies. The extended selection process takes consideration of the percentage of captured data and the percentage of existing outliers. Three different conditions have been introduced to determine the best outliers' condition to be used in a detailed analysis. The outliers are defined as follows:

$$\text{Outliers } 75\% = |\text{HsBuoy} - \text{HsCODAR}| > 75\,\%\,\text{HsBuoy} \quad (3)$$

$$\text{Outliers } 50\% = |\text{HsBuoy} - \text{HsCODAR}| > 50\,\%\,\text{HsBuoy} \quad (4)$$

$$\text{Outliers } 25\% = |\text{HsBuoy} - \text{HsCODAR}| > 25\,\%\,\text{HsBuoy} \quad (5)$$

Based on the outliers' percentage value, the useful data for range cell (RC) selection can be identified from the difference between the percentage of captured data and the percentage of outliers. Fig. 15 shows this analysis for December 2012. The RCs with the highest percentage of useful data were selected for qualitative analysis for outliers 75%, 50% and 25% in order to determine the most appropriate outliers' condition to be used to calculate useful data. Scatter plot (Fig. 16) were used to analyse correlation between useful data from the RCs and that from waverider buoy. A summary of the comparative analysis of root-mean square error (RMSE), coefficient of determination (R^2), bias and data counts from Fig. 18 is shown in Table 8. Based on these values, it is observed that outliers 50% (Eq. (4)) is the most appropriate to be used, as outliers 75% shows lower RMSE values, while outliers 25% shows lesser data counts.

The *Hs* values at selected RCs for the December 2012 period from the outliers 50% useful dataset were plotted against the average *Hs* values calculated across all the RCs and is shown in Fig. 17. Fig. 18 compares the averaged RC data against the waverider buoy data. Based on the comparison plots and comparative analysis shown in Table 8, it is observed that the dispersion of measured data across the selected RCs is rather small and the methodology of comparing average values of useful data from the identified RCs with Hs from waverider buoy is therefore justified. Table 9 shows a summary of the selected RCs for all analysis periods presented in this section.

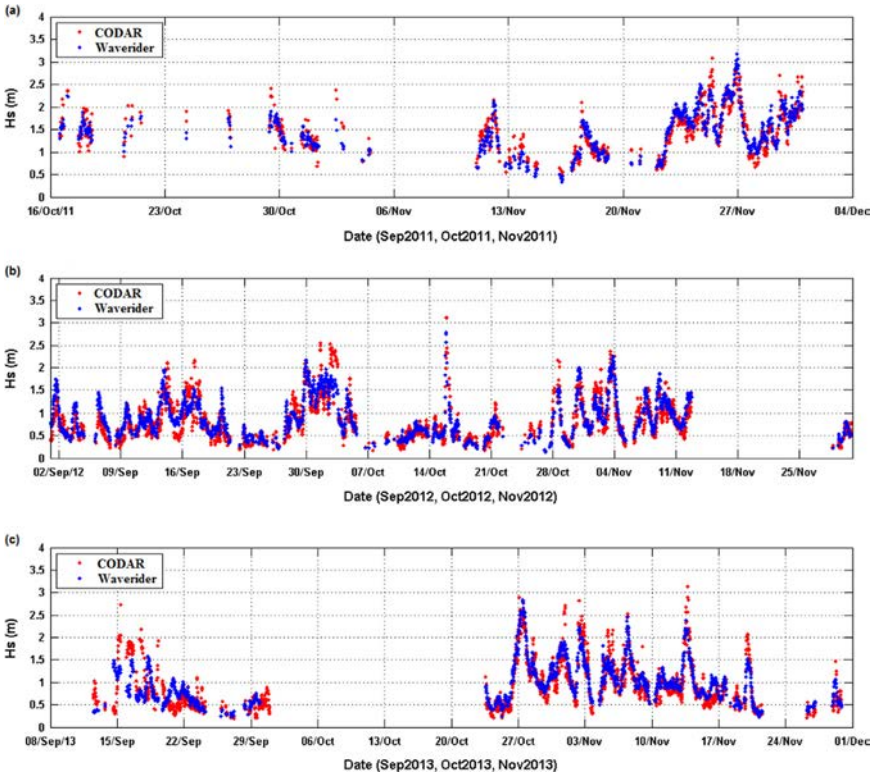

Fig. 21. Comparison of temporal variation of *Hs* between CODAR and wave buoy for autumn (a) 2011, (b) 2012 and (c) 2013.

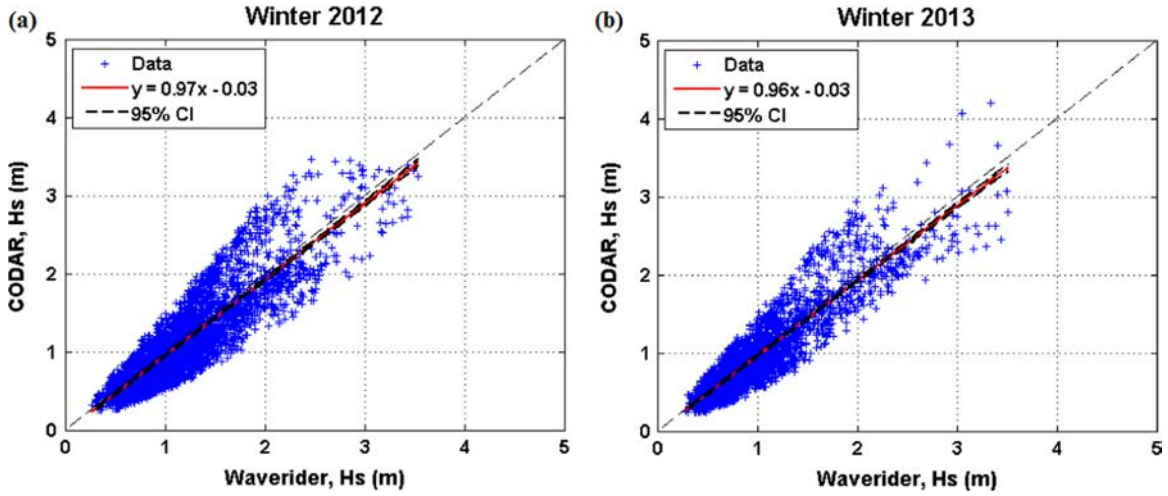

Fig. 22. Scatter plot comparison of *Hs* obtain from CODAR and wave buoy data for Winter (a) 2011 and (b) 2012.

4.2. Data comparisons

Figs. 19–21 show comparison plots between RC-averaged *Hs* from CODAR data against *Hs* obtained from the waverider buoy. The plots were divided into seasonal periods based on available CODAR data and it can be observed that the comparison plots show good agreement between the datasets. It is also observed that no data was available in April 2012 and less data was captured in the autumn period. Figs. 22–24 show seasonal scatter plots between data from CODAR and the waverider buoy. The plots confirm a good correlation between the datasets and statistical measures of correlation values such as RMSE, R^2 and bias are shown in Table 10. Based on these values, the CODAR *Hs* data is verified to be reliable for use in detailed of wave height characteristics and assessment of Galway Bay with alternative datasets.

4.3. Wave occurrences

Figs. 25–27 show the percentage of occurrence of waves of particular *Hs* from CODAR and waverider (see Fig. 3) where both data were available for winter, spring, summer and autumn period of 2011 to 2013. It is observed that, overall CODAR data shows similar *Hs* trends compared to waverider except for the autumn 2011 period. It is also clear that waves of higher amplitude occurred in the winter period where the *Hs* values exceed 4 m, while in spring and summer the maximum *Hs* values vary between 2 and 3 m and in autumn between 3 and 4 m. It is also observed that the most frequently occurring *Hs* were those between 0 and 1.5 m for all seasons with a total percentage of occurrences of between 50 and 85% compared to the other *Hs* ranges. Furthermore, the higher wave events that occurred in the range of 3–4 m in the winter period (i.e. 0.98% in winter 2012 and

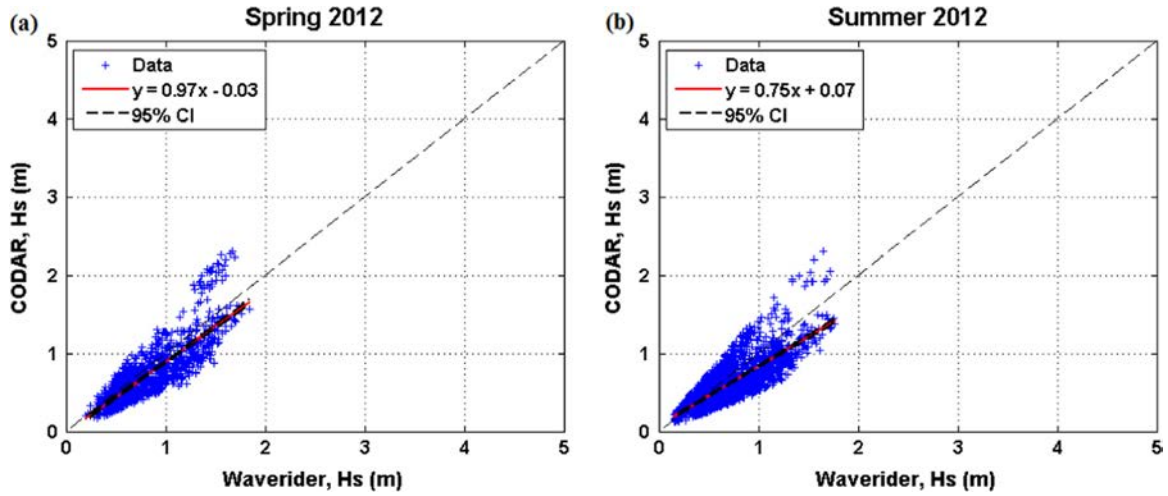

Fig. 23. Scatter plot of comparison of *Hs* obtain from CODAR and wave buoy data for Spring and Summer 2012.

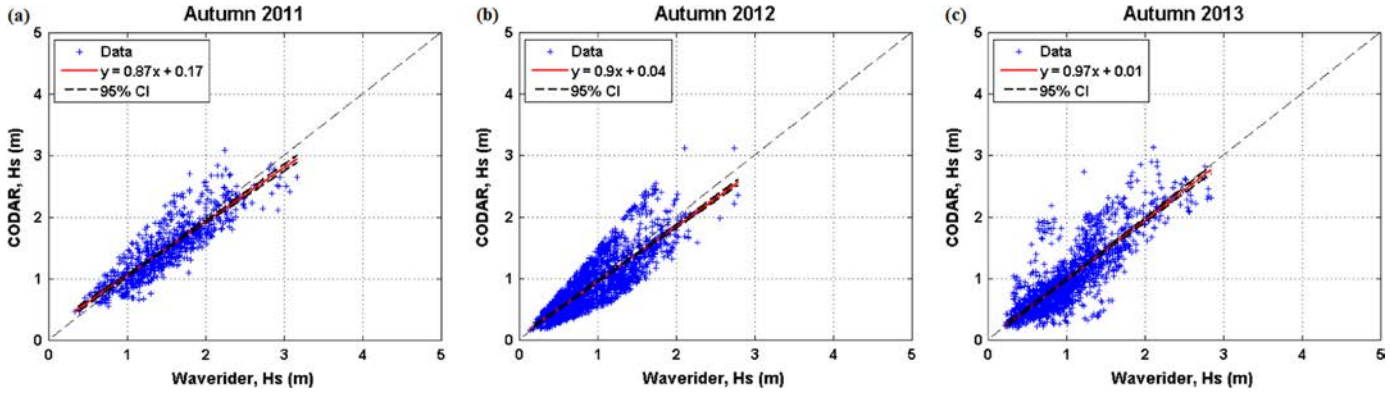

Fig. 24. Scatter plot of comparison of *Hs* obtain from CODAR and wave buoy data for Autumn 2011, 2012 and 2013.

Table 10
Summary of data correlation between CODAR and wave buoy data.

Period	Mean(m)	RMSE	R^2	Bias	Period	Mean(m)	RMSE	R^2	Bias
Winter 2012	1.15	0.29	0.75	0.09	Autumn 2011	1.46	0.24	0.76	0.06
Winter 2013	1.00	0.24	0.81	0.06	Autumn 2012	0.85	0.24	0.71	0.06
Spring 2012	0.73	0.21	0.70	0.04	Autumn 2013	0.95	0.30	0.69	0.09
Summer 2012	0.61	0.18	0.62	0.03					

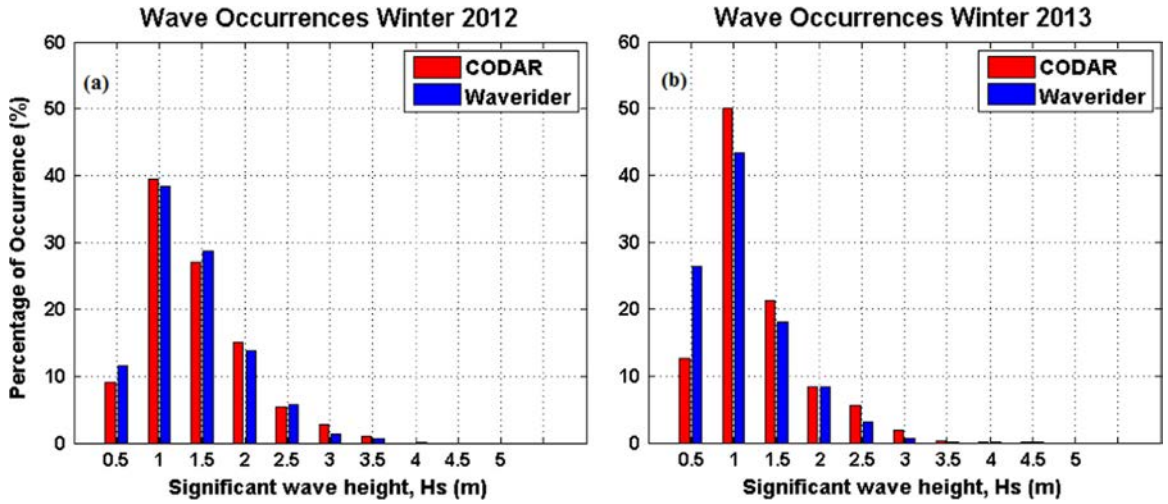

Fig. 25. Percentage of occurrence of average *Hs* determined from CODAR for Winter 2012 and 2013.

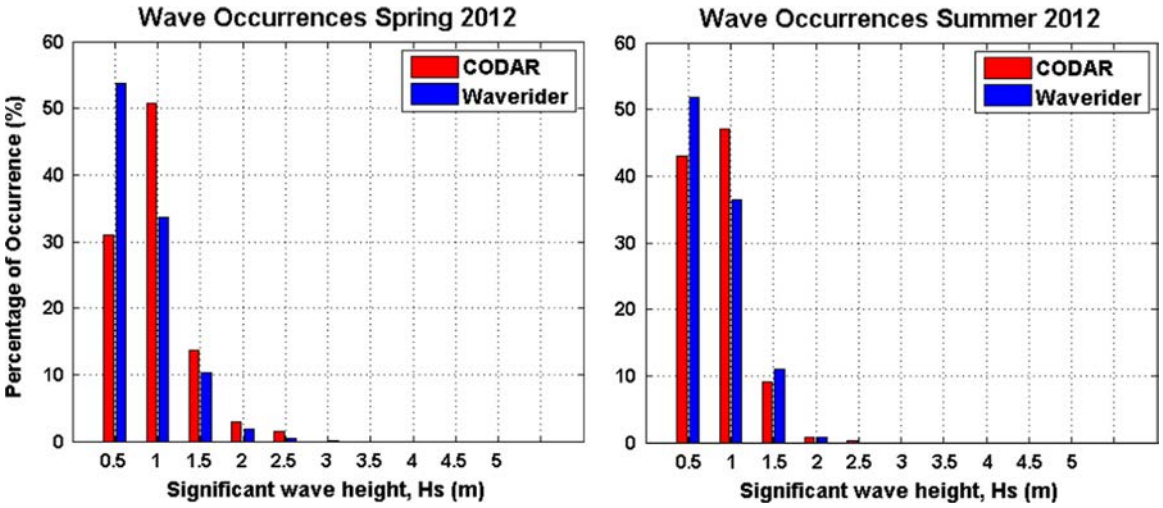

Fig. 26. Percentage of occurrence of average *Hs* determined from CODAR for Spring and Summer 2012.

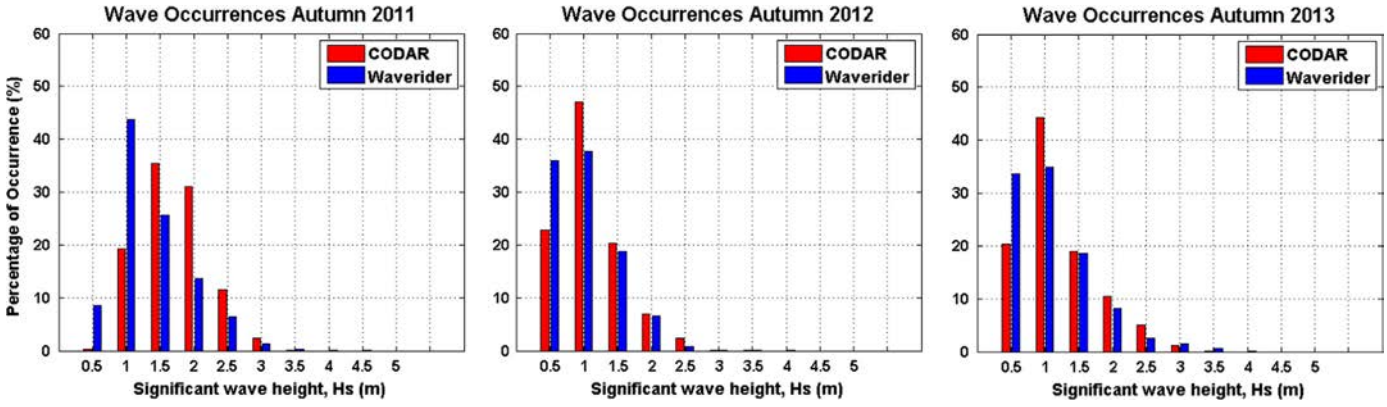

Fig. 27. Percentage of occurrence of average *Hs* determined from CODAR for Autumn 2011, 2012 and 2013.

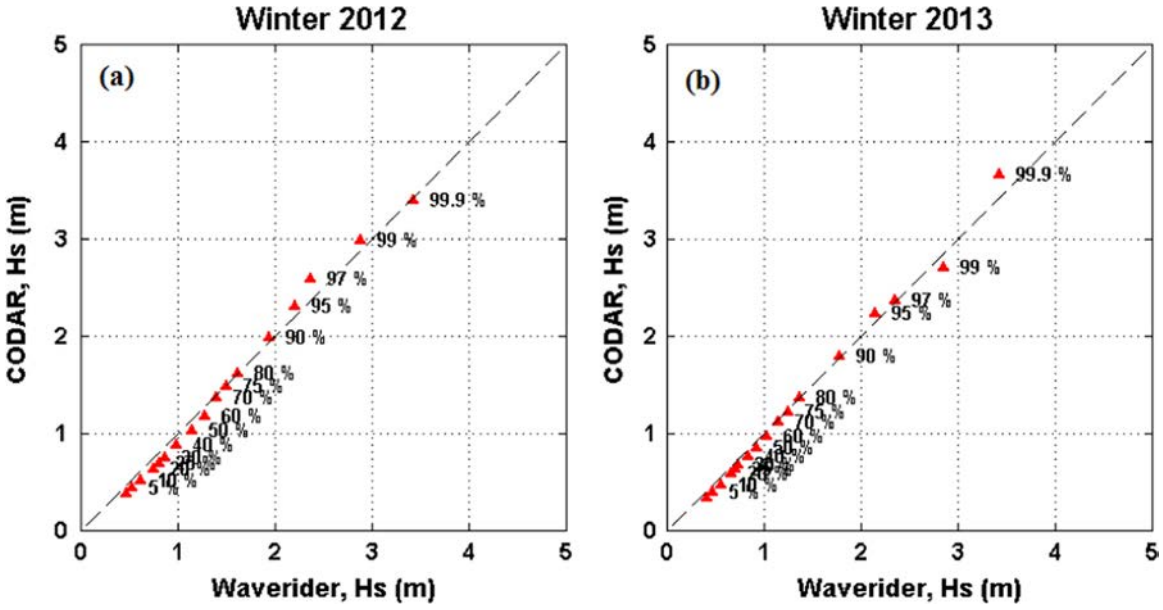

Fig. 28. QQ plot for significant wave heights, *Hs*, between CODAR and the wave buoy at Spiddal (Winter 2012 and 2013).

0.41% in winter 2013) were successfully captured by CODAR. It is also noted that less data was captured in the spring period which can be seen in Fig. 20(a). Furthermore, a significant difference in wave occurrences is observed in autumn 2011 compared to autumn 2012 and 2013. This is due to poor captured data as shown in Fig. 21(a). Thus, the percentage of wave occurrences for autumn 2011 is not dependable to be considered for wave height trends in autumn period. Discrepancies at lower wave heights (0–0.5 m) are a result of CODAR

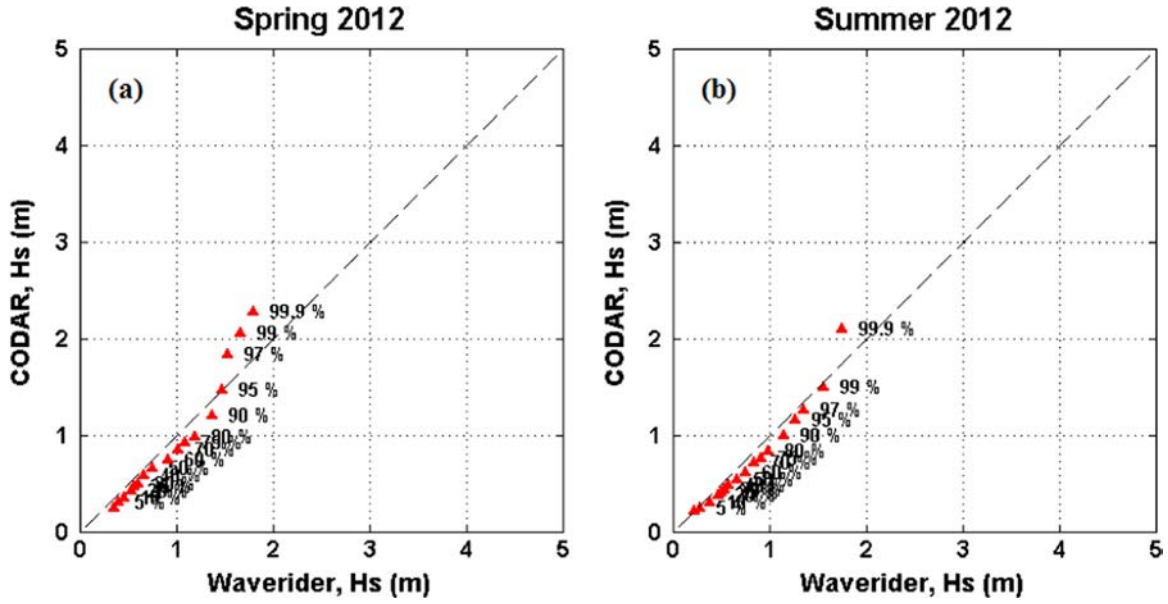

Fig. 29. QQ plot for significant wave heights, *Hs*, between CODAR and the wave buoy at Spiddal (Spring and Summer 2012).

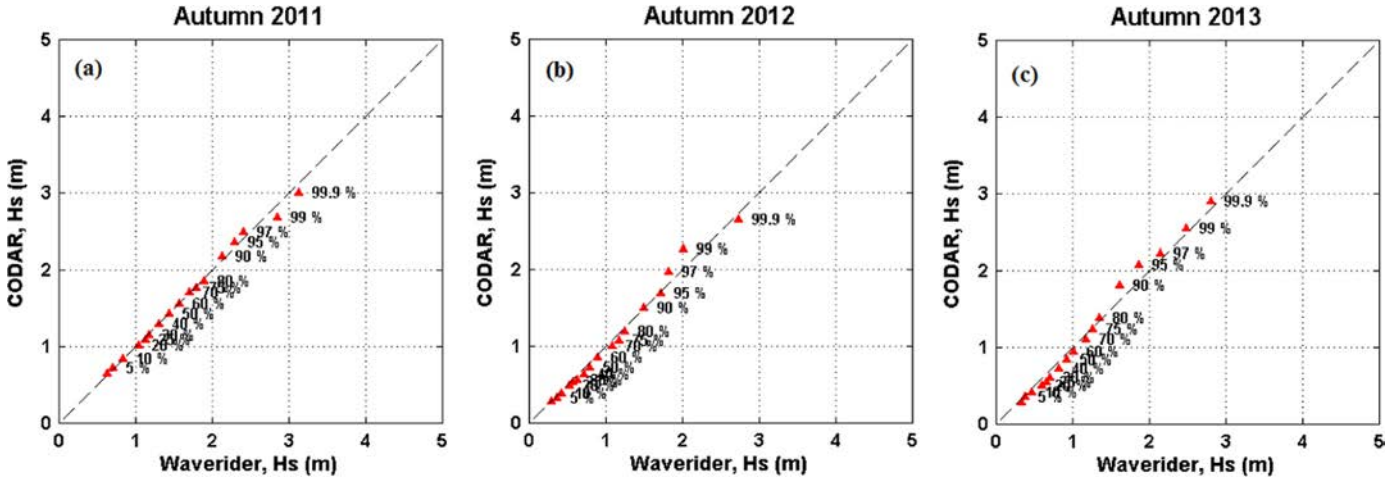

Fig. 30. QQ plot for significant wave heights, *Hs*, between CODAR and the wave buoy at Spiddal (Autumn 2011, 2012 and 2013).

requiring a rough sea surface for good data capture; in calmer sea states the radio waves may not be reflected and recorded resulting in poor data capture and erroneous readings. A detailed investigation on *Hs* assessment is continued with quantile–quantile plots (QQ plots) analysis in the next sub-section.

4.4. QQ plots

An extended approach to inspect *Hs* occurrence between CODAR data and waverider buoy is conducted by observing Quantile–quantile plots (QQ plots). QQ plots shows the quantiles of a first data set against the quantiles of a second dataset at specified quantiles and in this analysis, 5–99.9% quantiles were established. The purpose of using QQ plots is to determine the correlation and distribution of the two sets of wave data (CODAR and waverider buoy); the data points should fall approximately along a 1:1 relationship line if they are from two populations with the same distribution. The percentiles in QQ plots are calculated by sorting CODAR and waverider buoy data from a smallest to largest value and linear interpolation is used to compute percentiles for percent values. Figs. 28–30 show seasonal QQ plots for winter 2012 and 2013, spring 2012, summer 2012 and autumn 2011–2013, respectively. Overall, CODAR shows good agreement with the waverider data for all seasons and particularly for winter and autumn when the rougher sea states make for better quality CODAR measurements; this is indicated by the goodness of fit of data points with the 1:1 relationship line. It is observed in spring 2012, that CODAR data shows a significant difference from the 1:1 relationship line; this is due to there being less CODAR data captured in spring 2012 (see Fig. 20(a)). Looking, in particular, at the 90th and 99th quantiles used in Section 3.2.1 to characterise the upper threshold of operational wave heights and lower threshold of extreme wave heights, respectively, CODAR shows very good agreement with the wave rider (Figs. 30–32). Based on these QQ plots, it can be concluded that CODAR data is reliable to be used in assessments of *Hs* characteristics for the 1/4-scale test site but with the caveat that waverider buoy data is also required for determination of CODAR outliers.

4.5. Wind assessment

Wind is a dominant contributing factor to surface wave formation, ergo an assessment of the influence of wind magnitude and direction on wave occurrence was conducted. In the absence

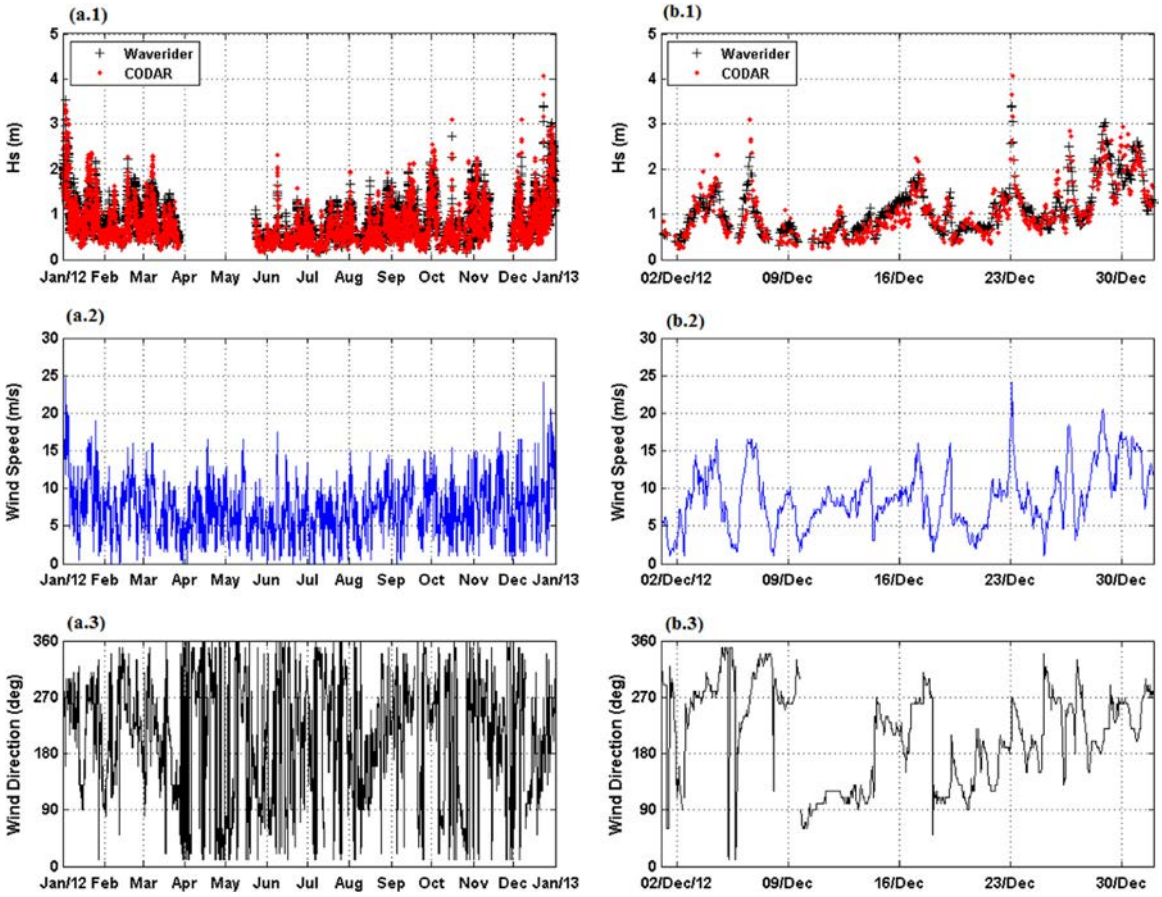

Fig. 31. Comparison plot of wind speed (m/s) and direction (degree) from Mace Head station with *Hs* (m) from CODAR and Wave buoy (2012) for (a) the full year of 2013 and (b) December 2013.

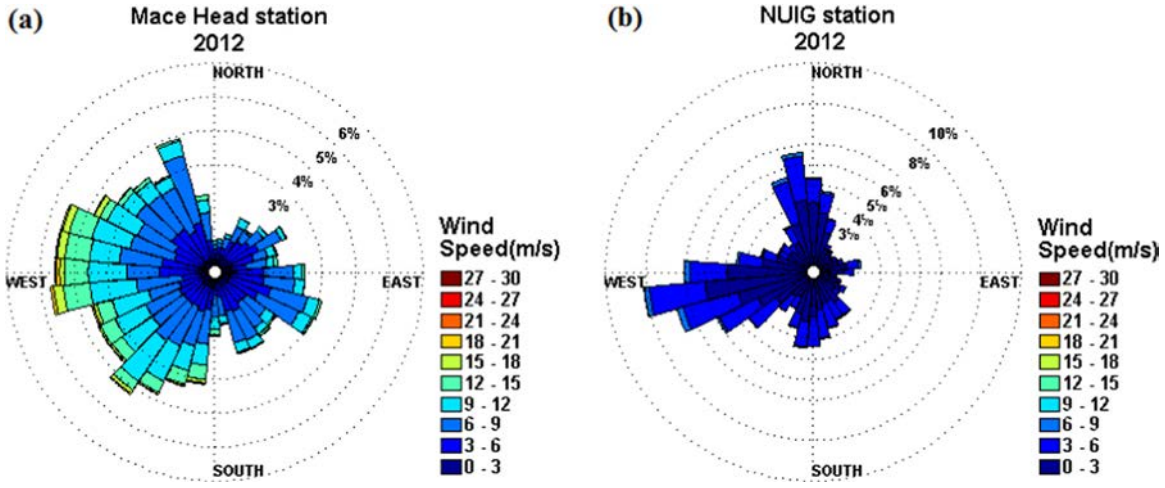

Fig. 32. Wind rose plot at (a) Mace Head and (b) NUIG station at 1 h interval (2012).

of site-specific wind data, two measured wind datasets were used in the assessment - the IRUSE weather station at NUIG and the Mace Head atmospheric research station (see Fig. 2). The straight line distance from the NUIG station to the test site is 5 km, while the distance from Mace Head station (−9.899E, −53.325N) is approximately 50 km. The measured wind data at NUIG station is taken from a weather station (−9.060E, 53.279N), which is owned and operated by the Informatics Research Unit for Sustainable Engineering, NUI Galway (IRUSE, 2015), while the Mace Head (MH) wind dataset is monitored and controlled by Atmospheric & Environmental Physics Cluster, School of Physics, NUI Galway (C-CAPS, 2015). The MH station is more exposed to the North Atlantic Ocean (clean sector, 180° through west to 300°) compared to NUIG station (on land at enclosed area). Thus, the wind characteristics captured at MH station are more reliable for use as a representative wind in this assessment.

Wind data was retrieved at one-hour time resolution for a period of a full year, 2012 (Éireann, 2015). Fig. 31(a.1)–(a.3) shows CODAR and waverider buoy , wind speed and wind direction plotted data for the year, while Fig. 31(b.1)–(b.3) shows a blown-up plot for December 2012. There appears to be a strong correlation between

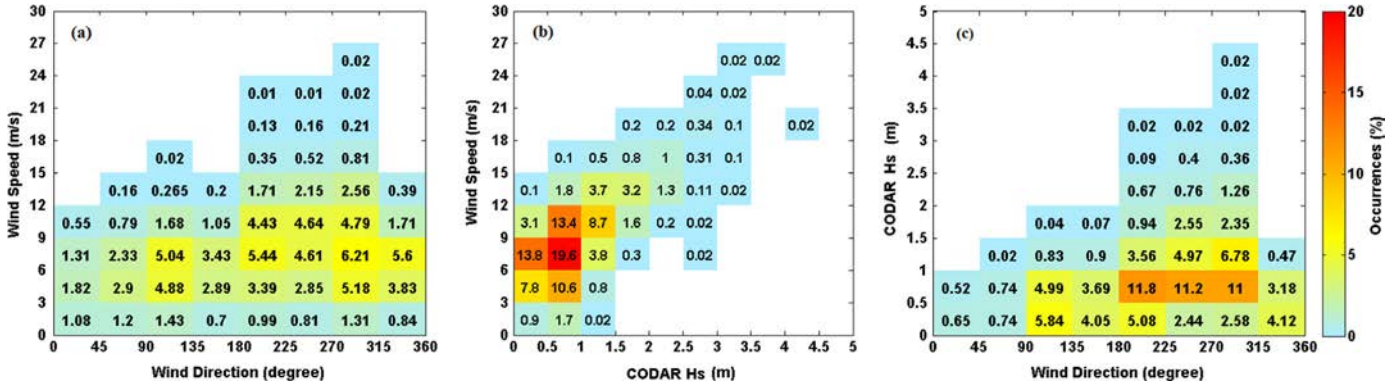

Fig. 33. (a) Percentage of occurrence at Mace Head station between wind speed (m/s) and wind direction (degree) for a year 2012, (b) Percentage of occurrence at Mace Head station between wind speed (m/s) and *Hs* (m) for 2012 and (c) Percentage of occurrence at Mace Head station between wind direction (degree) and *Hs* (m) for 2012.

wave height and wind speed indicating that the majority of waves at the site are wind waves. Based on the comparison plots, it is observed that higher waves occur simultaneously with stronger winds when the wind is blowing into the bay from the west, southwest and northwest. Where strong winds are blowing seaward from on shore, i.e. from between 10° and 150° with respect to the true North (meteorological convention), low wave heights are observed (e.g. 9–14 December 2012 in Fig. 31(b.2) and (b.3)). Fig. 32 shows wind rose plots at MH and NUIG stations for the period of 2012 and it is evident that the dominant wind is coming from west, southwest and northwest directions, but some strong wind events also come from the east, northeast and southeast sectors. Hence, average *Hs* CODAR patterns are observed to be represented from various winds. The percentage occurrence of wind speed and wind direction at Mace Head station for the 2012 period is shown in Fig. 33(a), while the percentage of occurrence between wind speed at Mace Head station and averaged *Hs* from CODAR data for 2012 is Fig. 33(b) and the percentage of occurrence between wind direction at Mace Head station and averaged *Hs* from CODAR data for 2012 is Fig. 33(c) . It is observed that strong winds result in higher wave events with dominant wave direction coming from 180 to 360 degree direction. For example, 19.6% of operational *Hs* between 1 m and 2 m occur during wind speeds of 6–9 m/s, while 0.2% of high wave events between 3 m and 5 m occurred when wind speeds range from 18 m/s to 27 m/s.

5. Conclusion

An assessment of wave characteristics at the 1/4 scale wave energy test site in Galway Bay is presented. The site was characterised using waverider data and a methodology developed by the authors. The methodology can be easily applied to any site, to any measured wave parameter, γ, and for any period of time and uses percentiles to specify clear threshold values for operational ($\gamma \leq$ 90th percentile), high (90th percentile $< \gamma \leq$ 99th percentile) and extreme ($\gamma >$ 99th percentile) wave events. Here, the methodology was applied separately to wave heights and wave power. Characterising the wave power available for a site is not only essential for predicting the operational performance of a wave energy convertor, but also for designing the device for survivability under high and extreme events. Characterisations in terms of wave heights and wave power were conducted for (1) a 5-year period from 2009 to 2013, (2) each individual year and (3) each individual seasonal. Following this, the accuracy of wave heights measured by a HF radar system was assessed for use in characterisation of a site by wave height. An approach for validating the accuracy of CODAR wave data is presented and wave height characterisations using CODAR data were compared with those made using waverider data. The following are the main conclusions drawn from the research:

- The wave climate at the 1/4 scale test site is predominantly locally wind-driven with some swell components coming in from the Atlantic Ocean.
- The annual mean wave heights and periods at the site ranged from 0.6 to 0.9 m and 4.0 to 4.2 s, respectively, while the maximum wave height and period recorded were 4.9 m and 8.2 s, respectively.
- The annual mean wave power at the site varied from 1.7 to 4.2 kW/m of wave crest with annual maximums ranging from 31.9 to 75.4 kW/m.
- As would be expected, given its geographical location on the north-eastern shore of the Atlantic Ocean, there is significant variability in wave height, period and power between seasons with autumn and winter periods being most energetic and summer being much less so. For example, the 5-year mean winter power availability was 3.3 kW/m compared to just 1.2 kW/m for summer.
- The 5-year characterisation by wave height classified operational waves as those with $Hs \leq 1.5$ m and extreme waves as those with $Hs > 2.5$ m while the characterisation by wave power classified operational waves as those with $P \leq 7$ kW/m and extreme waves as those with $P > 25$ kW/m. Due to the large inter-annual and seasonal variation in wave parameters at a site it is recommended that annual and seasonal characterisations be conducted as they were here.
- The characterisation methodology presented here should be extremely useful to wave energy device developers for optimising the performance and engineering design of their devices; they should also be useful to engineers for design offshore structure.
- The research found HF radar measured wave heights to be quite accurate compared to those measured by waverider; however, the radar data can contain some noise and a simultaneous set of measurements from an alternative source (in this case waverider) is required to filter the noise. Conducting a site characterisation by wave height using the CODAR data yielded very similar operational and extreme event thresholds to those obtained using waverider data. The advantage of having both HF radar and waverider deployed at the same location is that the HF radar gives spatial coverage, while the waverider is a point measurement.

Acknowledgements

This material is based upon works supported by the Science Foundation Ireland under Grant no. 12/RC/2302 through MaREI,

the National Centre for Marine Renewable Energy Ireland. Elements of the research were also supported by the MAREN2 and EnergyMARE Projects which are part-funded by the European Regional Development Fund (ERDF) through the Atlantic Area Transnational Programme (INTERREG IV). The first author gratefully acknowledges the receipt of the College of Engineering & Informatics Fellowship. The second author would like to acknowledge the support of Science Foundation Ireland through the Career Development Award Programme (Grant no. 13/CDA/2200).

References

Atan, R., Goggins, J., Hartnett, M., Agostinho, P., Nash, S., 2014. Assessment of extreme wave height events in Galway Bay using high frequency radar (CODAR) data, in: Proceedings of the 1st International Conference on Renewable Energies Offshore (RENEW). Lisbon, Portugal, 24–26th November.

Atan, R., Goggins, J., Nash, S., 2015. A preliminary assessment of the wave characteristics at the Atlantic Marine Energy Test Site (AMETS) using SWAN, in: Proceeding of the 11th European Wave and Tidal Energy Conference (EWTEC). Nante, France, 6–11th September.

Belinda, L., Nyden, B., 2005. Directional Wave Information from the SeaSonde. IEEE J. Ocean. Eng. 30, 70–80.

Cahill, B., 2013. Characteristics of the Wave Energy Resource at the Atlantic Marine Energy Test Site, PhD thesis. University College Cork, Ireland.

C-CAPS, 2015. Atmospheric & Environmental Physics Cluster Fifty Years of Measurements at Mace Head.

Cornett, A.M., 2008. A global wave energy resource assessment, in: The Eighteen (2008) International Offshore and Polar Engineering Conference. International Society of Offshore and Polar Engineers(ISOPE), Vancouver, Canada, 6-11th July, pp. 1–9.

DHI, 2012. Mike 21 by DHI [WWW Document]. URL ⟨⟨http://www.mikebydhi.com/products/mike-21/waves⟩⟩.

Fugro, 2014. World Wide Wave Statistics (WWWS) [WWW Document]. URL ⟨⟨http://www.oceanor.com/Services/WWWS⟩⟩.

Gulev, S.K., Gregorieva, V., 2006. Variability of the winter wind waves and swell in the North Atlantic and North Pacific as revealed by the voluntary observing ship data. Journal of Climate 19, 5667–5685.

Holthuijsen, L.H., 2009. Waves in Oceanic and Coastal Waters, 2009th ed. Cambridge University Press, New York, United State of America.

IRUSE, 2015. IRUSE : Informatics Research Unit For Sustainable Engineering [WWW Document]. URL ⟨⟨http://www.iruse.ie/⟩⟩.

Marine Institute, 2015. Data.Marine.ie : Wave Buoy Network Real Time Data 30 Minute [WWW Document]. Mar. Inst. URL ⟨⟨http://data.marine.ie/Dataset/Details/20969#⟩⟩ (accessed 1.20.15.).

Met Éireann, 2014. Met Eireann Weather News : Another record wave height set today south of Cork [WWW Document]. MET ÉIREANN, Glas. Hill, Dublin 9, Irel. URL ⟨⟨http://www.met.ie/news/display.asp?ID=243⟩⟩ (accessed 12.15.14.).

Met Éireann, 2015. Met.ie,The Irish Meteorological Service Online,Download Historical Climate Data for our Synoptic Stations [WWW Document]. MET ÉIREANN, Glas. Hill, Dublin 9, Irel. URL ⟨h⟨ttp://www.met.ie/climate-request/⟩⟩ (accessed 1.27.15.).

Coe R.G., Neary V.S., 2014. Review of Methods for Modeling Wave Energy Converter Survival in Extreme Sea States, Proc 2nd Mar Energy Technol Symp (METS), Seattle, WA, USA. http://hdl.handle.net/10919/49221.

O'Brien, L., Dudley, J.M., Dias, F., 2013. Extreme wave events in Ireland: 14 680 BP–2012. Nat. Hazards Earth Syst. Sci. 13, 625–648. http://dx.doi.org/10.5194/nhess-13-625-2013.

OES, 2015. Ocean Energy Systems (OES), Ocean Energy in The World : Offshore Installations Worldwide [WWW Document]. OES-Ocean Energy Syst. URL ⟨⟨http://www.ocean-energy-systems.org/ocean-energy-in-the-world/gis-map/⟩⟩ (accessed 2.24.15.).

Pandian, P.K., Emmanuel, O., Ruscoe, J.P., Side, J.C., Harris, R.E., Bullen, C.R., 2010. An overview of recent technologies on wave and current measurement in coastal and marine applications. J. Oceanogr. Mar. Sci. 1, 1–10.

Qualitas, 2015. Qualitas Remos : Technology solutions and services for a safe and sustainable marine environment.

Tolman, H.L., 1991. A third-generation model for wind waves on slowly varying, unsteady and inhomogeneous depths and currents. J. Phys. Oceanogr. 21, 782–795.

TUDelft, 2014. SWAN Implementation Manual - Cycle III version 41.01 [WWW Document]. Delft Univ. Technol. URL ⟨⟨http://swanmodel.sourceforge.net/online_doc/swanimp/swanimp.html⟩⟩ (accessed 1.17.14.).